



***In silico* Identification of bioactive compounds from *Chasmanthera dependens* and *Carissa edulis* as potential inhibitors of Carbonic anhydrases (CAs) receptors using a target-based drug design approach**

**Abayomi Dele Owonikoko¹, Abiodun Sodamade¹, Abimbola Modupe Olatunde²,
Oluwatoyin Funke Odoje¹ and Banjo Semire³**

¹Department of Physical Sciences Education, Emmanuel Alayande University of Education, Oyo. Oyo State, Nigeria.

²Department of Chemistry University of Ibadan, Ibadan. Oyo State, Nigeria.

³Department of Pure and Applied Chemistry, Ladoke Akintola University of Technology, Ogbomoso. Oyo State, Nigeria.

Abstract

Epilepsy is a brain disorder that affects over 65 million people around the globe. Despite the availability of anti-epilepsy drugs, the war against this unmet medical condition is yet to be resolved. Most epilepsy patients are resistant to available anti-epilepsy medications coupled with the strong side effects of these drugs, thus the need for an alternative therapy that is affordable. The therapeutic roles of bioactive compounds from medicinal plants against many diseases can never be over-emphasized for their potency, efficacy, and safety. This arouses our interest to assess the anti-epileptic ability of bioactive compounds from *Chasmanthera dependens* and *Carissa edulis* using an *in-silico* drug design approach. In the current study, ninety-nine (99) phytochemicals from *Chasmanthera dependens* and *Carissa edulis* were screened against Carbonic anhydrases (VII and XIV) drug targets through ADMET profile, PASS and molecular docking. The results identified seven (7) compounds vis-à-vis Bisnorargemone (C6), Catechin (C13), Columbamine (C16), Coreximine (C18), Pallidine (C36), Salicin (C45) and alpha-carissanol (C49) for both CA VII and CA XIV receptors. These selected leads could probably be strong inhibitors of the targets due to their favourable binding affinities, interactions with the targets at the active sites, excellent ADMET profiles, PASS and physicochemical properties than Lacosamide and Acetazolamide, used as standard drugs. Thus, the seven identified lead compounds can be candidates for further investigations for the development of new anti-epilepsy medications.

Keywords

Epilepsy, Phytochemicals, Carbonic anhydrases, ADMET, Computer Aided Drug Design, Antiepileptic Drugs (AEDs)

1.0 Introduction

Epilepsy, a chronic, recurring and progressive neurological condition that affects the brain remains an unmet medical disease that needs urgent attention. It affects over 65 million people of all ages worldwide (Zavala-Tecuapetla et al. 2020; Devinsky et al. 2018), with higher cases in men than in women (Beghi, 2020). As opined by the International League against Epilepsy (ILAE), epilepsy is characterized as two or more unprovoked seizures occurring an average of 1440 seconds apart, or one unprovoked seizure occurring when the likelihood of another is higher than 60% (Ciccone et al. 2021). Seizures are either focal or generalized. A focal seizure takes place at a particular region of the brain, thus, the brain areas where the synchronous firing of a neuronal cell group takes place determine the behavioural outcome. On the other hand, the cerebral hemispheres which are spread via connections between the thalamocortical

regions are involved in generalized seizures (Sarmast et al. 2020). Moreover, social prejudice against epilepsy patients and their loved ones and lack of necessary care as a result of many cultural and financial challenges have affected the war against epilepsy, especially in Africa (Ciccone et al. 2021), and the severe effects of this condition on world health have led scientists and researchers to continuous action to understand the intricate mechanisms underlying seizure genesis and to create effective pharmaceutical treatment plans for epilepsy (Ciccone et al. 2021).

However, despite the availability of antiepileptic drugs (AEDs), many epilepsy patients remain uncured as 30% of all patients have drug-resistant epilepsy (Kalilani et al. 2018), i.e. there is persistence of epileptic seizures despite the use of an acceptable and well-tolerated pharmacological treatment (Kwan et al. 2009). There are only a few kinds of epilepsy that antiepileptic drugs (AEDs) may cure, even though the pharmacological treatment is frequently ineffective (Löscher et al. 2020). Also, the most prevalent type of epilepsy, temporal lobe epilepsy (TLE), is frequently resistant to AEDs (Engel, 2001; Kwan, 2004), and the pathophysiological mechanisms underlying the occurrence remain unresolved, although, Pitkänen and Lukasiuk (2011) hypothesized that the development of the disorder most likely involves a combination of neurological changes in the brain. Therefore, the identification of novel molecular targets and lead is urgently required to increase therapeutic options for the treatment of this unmet medical need.

Carbonic anhydrases (CAs) play an indispensable role in epilepsy therapy. They are metalloenzymes that catalyze the reversible hydration or dehydration of $\text{CO}_2/\text{HCO}_3^-$ and participate in physiological and pathological processes where cellular pH buffering is of great significance. Sixteen distinct isoforms of α -CAs are well documented in humans, each with a unique catalytic activity as well as a different sub-cellular and tissue distribution. However, the CAs II, VII, and XIV have reportedly been linked to epilepsy (Aggarwal et al. 2013; Mishra et al. 2020; Ozsoy et al. 2021; Ciccone et al. 2021). A zinc ion (Zn^{2+}) plays a pivotal role in the catalytic activity of α -CAs active site (Supuran, 2010). It controls CO_2 tissue content and cellular pH buffering by catalyzing the reversible hydration or dehydration of $\text{CO}_2/\text{HCO}_3^-$. Recent research has amply shown that low CO_2 levels and alkalosis increase neural excitability, and sustain seizure generation (Tong, 2000; Leniger et al., 2004; Ruusuvaari and Kaila, 2014).

Moreover, evidence from the literature has established the role of bioactive compounds in the quest for the discovery and development of novel and effective medication in the treatment of several life-threatening medical conditions. Saponins, tannins, flavonoids, phytosterols, and alkaloids have been identified as possible inhibitors of the main protease (M^{pro}) of the SARS-CoV-2 virus (Oyebamiji et al., 2020; Adegbola et al., 2021; Falade et al. 2021; Abdul-Hammed et al. 2021). Similarly, Cyanidine, Lupeol, and Phloretin-2-O-beta glucoside, obtained from the *Phyllanthus niruri* have been recommended for further development in the quest of designing novel anti-hepatitis C therapy (Adedotun et al. 2022). These aroused our interest to explore phytochemicals isolated from *Chasmanthera dependens* and *Carissa edulis* whose medicinal prowess in treating various diseases traditionally including epilepsy has been established (Yaro et al., 2015). Also, lead identification and optimization are very important in the early stage of drug discovery and development, and Computer Aided Drug Design (CADD) has been an indispensable tool in the identification of probable lead compounds (Abdul-Hammed et al., 2021). Therefore, this research focused on the investigation of the inhibitory potential of isolated compounds from *Chasmanthera dependens* and *Carissa edulis* against the CAs (VII and XIV) drug targets using the CADD approach.

2.0 In silico Methods

2.1 Preparation of Target Receptors (Carbonic anhydrases VII and XIV)

The 3D crystal structure of Carbonic anhydrases (CAs) target receptors (CA VII and XIV) with PDB IDs (3ML5 and 4LU3) were downloaded from the protein databank (PDB) (<https://www.rscb.org>). The downloaded structures were treated to remove water molecules and unwanted molecular interactions during the docking simulation using BIOVIA, 2019 Discovery Studio. The Ramachandran plots of the two receptors were carried out to validate their qualities (Ramachandran and Sasisekharan, 1968) and the binding pockets of the initial inhibitors present in the receptors were used to determine the binding parameters for X, Y, and Z coordinates respectively.

2.2 Preparation of Ligands and Equilibrium Geometry Optimization

PubChem database (<https://pubchem.ncbi.nlm.nih.gov>) was explored for the 2D/3D structures of the isolated phytochemicals (ligands) from *Chasmanthera dependens* and *Carissa edulis* (Table 1a and 1b). Spartan 14 software was used to convert all the 2D structures downloaded to 3D. These were followed by a conformer search operation using Molecular Mechanics Force Field (MMFF)

and equilibrium geometry optimization using the Density Functional Theory Method (DFT) at B3LYP with 6-31+G* as a basis set (Hegre, 2011). The optimized ligands were used for protein-ligand docking operations

2.3 Determination of Receptors Active Sites

The active sites of the two target receptors were assessed using Biovia Discovery Studio and Computed Atlas for Surface Topology (CASTp) (BIOVIA, 2019; Tian et al. 2019) and were verified and validated using the source journal obtained protein data bank.

2.4 ADMET Profiling of the Ligands

ADMETSar2 web server (<http://immd.ecust.edu.cn/admetSar2/>) (Yang et al. 2019) was used to investigate the absorption, distribution, metabolism, excretion, and toxicity (ADMET) of the ligands.

2.5 Drug-likeness, Lead-likeness and Oral-bioavailability Analyses

The drug-likeness properties of the studied ligands were analyzed using Molecular Inspiration's Lipinski filter while the SwissADME web server (<http://www.swissadme.ch/>) (Daina et al. 2017) was used to determine the lead-likeness and oral-bioavailability of the studied ligands.

2.6 Prediction of Activity Spectra for Substances (PASS)

The anti-epilepsy biological activities of the studied compounds were predicted using the PASS online web server (Goel et al. 2011).

2.7 Protein-Ligand Molecular Docking Operation and Visualization

The target docking operations were performed using the reliable (PyRx) docking software in triplicate. The average mean and standard deviations of each protein ligand were calculated to determine the binding affinities of each of the studied complexes. The inhibition constant (K_i) was calculated using equations 1 or 2, and the docked complexes' intermolecular interactions (such as hydrophobic, hydrogen bonds, halogen bonds, and /or aromatic interactions) were visualized using Accelrys Discovery Studio Visualizer 4.1 (DS)

$$K_i = \exp(\Delta G / RT) \dots (1)$$

$$\Delta G = -RT \ln K_i \dots (2)$$

Where R = Gas constant (1.987×10^{-3} kcal/mol); T = 298.15 K (absolute temperature); K_i = Inhibition constant and ΔG = Binding energy.

Table 1a List of studied phytochemicals from *Carissa edulis*

S/N	Phenolic acid and Flavonoids	S/N	Terpenoids
1	kaempferol 3-O-β-d glucopyranoside	41	carassin
2	quercetin-3-O-β-d glucopyranoside	42	carandoside
3	isorhamnetin-3-O-β-d-glucopyranoside	43	α-amyrin
4	caffeic acid methyl ester	44	lupeol
5	kaempferol	45	β-amyrin
6	rutin		Steroids
7	pinitol	46	β-sitosterol
8	naringin	47	stigmaterol glucoside
9	2-hydroxyacetophenone	48	20-Hydroxypregnan 18-oic acid
10	kaempferol-3-O-robinobioside	49	Stigmaterol
11	variabiloside E	50	Betulinic acid
12	p-coumaric acid	51	Carandinol
13	Salicin	52	Odoroside H
14	hydroxybenzoic acid		Sesquiterpenes
15	Coniferaldehyde	53	Dehydrocarissone
16	Catalponol		Lignans
17	Quinic acid	54	Olivil
18	Citric acid	55	(-)-Secoisolariciresinol
19	Neochlorogenic acid	56	(+)-Cycloolivil
20	Chlorogenic acid	57	8-hydroxypinoresinol
21	Cryptochlorogenic acid	58	(+) Pinoresinol
22	Catechin	59	(+)-lariciresinol

23	Quercetin-3-O-glucosyl-xyloside	60	–(–)-nortachelogenin
24	Quercetin-3-O-robinobioside	Sterols and triterpenes	
25	Quercetin-3-O-glucoside (isoquercitrin)	61	Carindone
26	Dicaffeoylquinic acid	62	Carenone
27	1-{ 1-[2-(2 hydroxypropoxy) propoxy] propan-2-yloxy} propan-2-ol	Coumarins	
28	Peonidin 3-rutinoside	63	Scopoletin
29	Oleuropein	64	Odoraside F
Terpenoids		65	Ononitol
30	Carinol	66	isofraxidin
31	Carissone	Condensed tannins/procyanidin	
32	cryptomeridiol	67	Procyanidin dimer
33	β-eudesmol	68	Procyanidin trimer
34	germacrenone		
35	carissanol		
36	6α-carissanol		
37	α-carissanol		
38	carissic acid		
39	oleanolic acid		
40	ursolic acid		



Table 1bList of studied phytochemicals from *Chasmanthera dependes*

S/N	Quaternary Alkaloids (In the stem bark)	S/N	Tannins
69	Jateorrhizine	87	Gallotannins
70	palmatine (berbericine)	88	Ellagitannins
71	columbamine	89	proanthocyanidins
72	pseudocolumbamine		Tertiary phenolic alkaloids
73	magnoflorine	90	Columbin
	Tertiary Non-Phenolic Alkaloids		Diterpenoid (stem, leaf and root)
74	Anonaine	91	Berberine
75	Glaucine		Essential oil (fatty acid)
76	Norglaucine	92	n-hexadecanoic acid
77	oxoglaucine	93	oleic acid
78	nornuciferine	94	tetradecanoic acid
79	govanine	95	heptadecanoic acid
80	coreximine (tetrahydroprotoberberine)	96	pentadecanoic acid
81	bisnorargemonine	97	estra-1,3,5 (10)-trien-17-ol
82	morphinandienone	98	9,17-octadecadienal (Z)
83	Liriodenine	99	13-heptadecyn-1-ol
84	lysicamine (oxonucliferine)		
85	Pallidine		
86	tetrahydropalmatine		

3.0 Results and Discussion

3.1 Validation of Target Receptors and Active Site Analysis

Carbonic anhydrases (CAs) are zinc metallozymes found in most living organisms and are known to catalyze the reversible hydration of CO₂ to bicarbonate (Krishnamurthy et al. 2008, Sippel et al. 2009; Alterio et al. 2013). Human Carbonic Anhydrase VII (CA VII) is a cytosolic member of α -CA enzymes which is mainly found in several brain tissues such as the hippocampus, cortex, and thalamus. It is known for generating neuronal excitation and seizures and is also involved in neuropathic pain control, thus, its inhibition is essential in eliminating neuronal excitation-associated seizures (Di Fiore et al. 2010). The 2.05 Å X-ray crystallographic structure (PDB: 3ML5) is a mutated form of human CA VII in complex with a classical sulfonamide inhibitor i.e. acetazolamide (AZM). It is a monomeric compact globular receptor with 269 amino residues and an ovoidal shape of approximately 40 x 40 x 40 Å³. It consists of a central 10-stranded β -sheet surrounded by four α - and four 3_{10} - helices and five additional β -strands (Di Fiore et al. 2010). Its Ramachandran properties include 0% outlier, 88.2% most favoured region, and 11.8% additional allowed regions (Fig. 1a). The active site (Fig. 1b) of the MCA VII complex with AZM is situated in a conical cavity about 15 Å wide and 15 Å deep, which spans from the surface of the protein to the centre of the molecule. The catalytic zinc ion is located at the bottom of this cavity, coordinated by three histidine residues. The fourth coordination position is occupied by the deprotonated sulfonamide NH group of the AZM inhibitor which co-crystallized with the enzyme and shows the main protein-inhibitor interactions. The amino residue in this active site include Gln92, His94, His96, His119, Val121, Phe131, Val143, Leu198, Thr199, Thr200, and Trp209.

Similarly, Human Carbonic anhydrase XIV (CA XIV) is the last member of the human CA family localized in the brain, kidneys, small intestine, urinary bladder, liver, and spinal cord (Alterio et al. 2013). It is a membrane-associated enzyme with an N-terminal extracellular domain, a putative transmembrane region, and a small cytoplasmic tail. Thus, its inhibition will aid the discovery of effective and highly economical drugs for the treatment of epilepsy. The crystal structure of Human Carbonic anhydrase (CA XIV) PDB ID: 4LU3 is a 279 sequence length non-mutated receptor with 2.00Å resolution, Ramachandran (Figure 2a) outlier of 0%, most favoured region of 90.2% and additionally allowed region of 9.8%. The residue in the active site (Figure 2b) of 4LU3 are Gln92, His94, His96, Gln106, Ala135, His119, Leu198, Thr199, Pro201, Trp209, Val121, Leu141, Phe131, Val143, and Thr200.

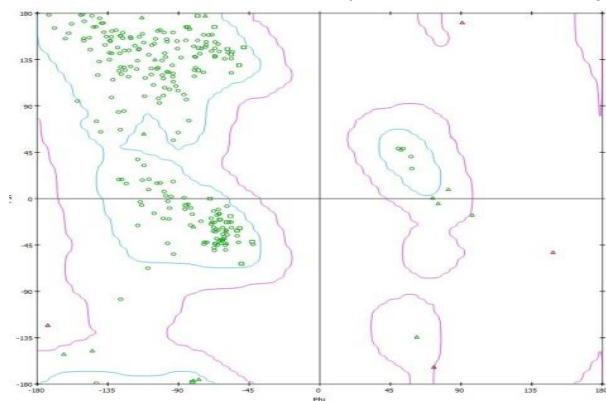


Fig. 1a The Ramachandran plot of Mutated Human Carbonic Anhydrase VII (CAVII) (PDB ID: 3ML5)

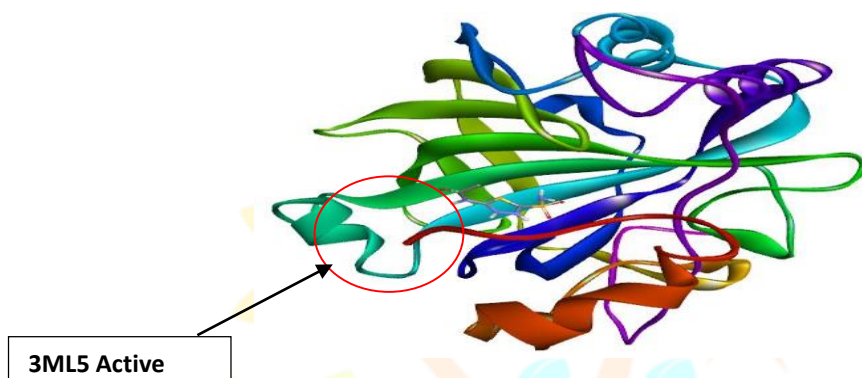


Fig. 1b The Crystal Structure of Mutated Human carbonic anhydrase VII (CAVII) (PDB ID: 3ML5) complexed with inhibitor acetazolamide (AZM) showing the receptor active site.

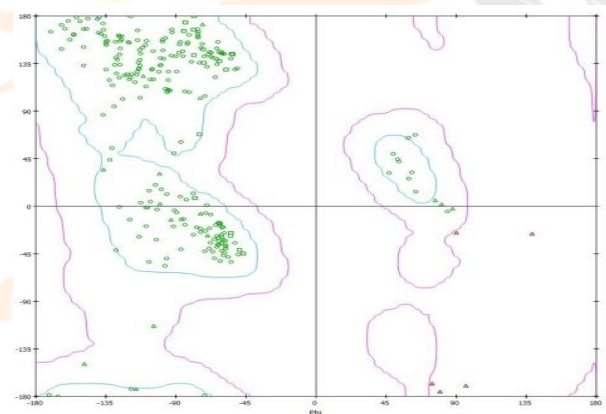


Fig. 2a The Ramachandran plot of Human Carbonic Anhydrase XIV (CA XIV) (PDB ID: 4LU3)

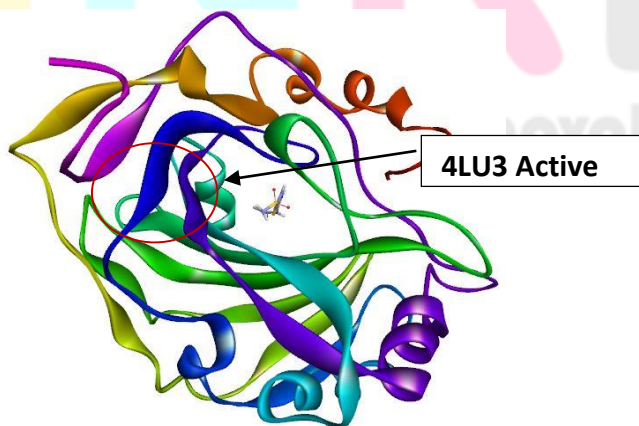


Fig. 2b The Crystal Structure of Human carbonic anhydrase XIV (CA XIV) (PDB ID: 4LU3) complexed with inhibitor acetazolamide (AZM) showing the receptor active site.

3.2 ADMET Analysis of the Studied Ligand

Half of the drug candidates failed at clinical due to poor and unacceptable ADMET properties. In other to prevent time and resource wastage (Guan, et al. 2018), investigating the Absorption, Distribution, Metabolism, Excretion and Toxicity (ADMET) profile of the potential drug molecule became an indispensable operation in drug design. This is also to ensure excellent efficacy and potency of the probable drug molecule with favourable ADME and toxicity properties as the required dosage is met (Adegbola et al., 2021; Adedotun et al. 2022). In this analysis, well-validated and highly used ADMETSAR2 web server (<https://lmmd.ecust.edu.cn/admetsar2/>) (Yang et al. 2019) was used to investigate the ADMET properties of ninety-nine (99) highly optimized isolated phytochemicals from *Carissa edulis* and *Chasmanthera dependes*, six (6) commercial anti-epilepsy drugs (S1-S6) and one (1) native inhibitor, a co-factor (acetazolamide (AZM) (S7). The results of the successful ligands with acceptable ADMET properties are shown in **Tables 2a and 2b**.

Table 2a ADMET profiling of the selected ligands and standard drugs

Absorption and distribution										
	C1	C2	C3	C4	C5	C6	C7	C8	C9	C10
BBB(±)	+0.7250	-0.5250	+0.9500	+0.7000	+0.5750	+0.5750	-0.6750	+0.6750	+0.7250	+0.8000
HIA +	+0.7571	+0.9956	-0.6429	+0.9927	+0.7454	-0.6286	+0.9726	+0.9970	+0.9954	-0.5571
Aqueous Solubility(LogS)	-0.421	-3.493	-1.579	-3.556	-2.974	-2.95	-2.07	-4.139	-2.168	-3.599
Metabolism										
CYP450C19 Inhibitor	0.9051 Non-inhibitor	0.8007 Inhibitor	0.8924 Non-inhibitor	0.9460 Non-inhibitor	0.7463 Non-inhibitor	0.7144 Non-inhibitor	0.8035 Non-inhibitor	0.8829 Non-inhibitor	0.7075 Non-inhibitor	0.8657 Non-inhibitor
CYP450 1A2 Inhibitor	0.5168 Non-inhibitor	0.7796 Non-Inhibitor	0.5069 Non-Inhibitor	0.7752 Inhibitor	0.9107 Inhibitor	0.7283 Inhibitor	0.7902 Non-inhibitor	0.5611 Inhibitor	0.5768 Non-inhibitor	0.6194 Non-inhibitor
CYP450 3A4 Inhibitor	0.9612 Non-inhibitor	0.7979 Non-Inhibitor	0.8566 Non-inhibitor	0.8759 Inhibitor	0.5873 Non-inhibitor	0.8177 Non-inhibitor	0.9238 Non-inhibitor	0.9227 Non-inhibitor	0.9443 Non-inhibitor	0.7618 Non-inhibitor
CYP450 2C9 Inhibitor	0.9051 Non-inhibitor	0.7602 Non-inhibitor	0.7824 Non-inhibitor	0.8754 Inhibitor	0.9070 Non-inhibitor	0.8824 Non-inhibitor	0.7471 Non-inhibitor	0.8749 Non-inhibitor	0.8084 Non-inhibitor	0.8043 Non-inhibitor
CYP450 2D6 Inhibitor	0.9602 Non-inhibitor	0.9378 Non-inhibitor	0.9275 Non-inhibitor	0.9624 Non-inhibitor	0.8933 Inhibitor	0.7749 Inhibitor	0.9654 Non-inhibitor	0.9705 Non-inhibitor	0.9003 Non-inhibitor	0.9440 Non-inhibitor
Excretion										
Biodegradation	0.7500 B	0.7000 NB	0.6500 B	0.7250 NB	0.9000 NB	0.9500 NB	0.5250 B	0.8500 NB	0.6250 B	0.8750 NB
Toxicity										
AMES Mutagenesis	0.9000 Non-Ames toxic	0.6982 Non-Ames toxic	0.9900 Non-Ames toxic	0.7500 Non-Ames toxic	0.7300 Non-Ames toxic	0.8100 Non-Ames toxic	0.7900 Non-Ames toxic	0.8200 Non-Ames toxic	0.8800 Non-Ames toxic	0.7400 Non-Ames toxic
Acute Oral Toxicity	0.7668 III	0.3999 III	0.4179 III	0.6545 III	0.6360 III	0.6317 III	0.6051 IV	0.8606 III	0.7646 III	0.3967 III
Eye irritation (YES/NO)	Yes	No	Yes	No	No	No	Yes	No	Yes	No
Eye corrosion (YES/NO)	No	No	Yes	No	No	No	No	No	No	No
hERG inhibition	0.8902 No	0.8235 No	0.5874 No	0.8063 No	0.7260 No	0.5000 No	0.7071 No	0.5514 No	0.7172 No	0.4780 No
Hepatotoxicity	0.5052 Yes	0.5419 Yes	0.5257 No	0.6129 No	0.6250 Yes	0.6375 No	0.6553 No	0.7260 No	0.7407 Yes	0.5625 No

© 2024 IJNRD Volume 9, Issue 7 July 2024 ISSN: 2456-4184 IJNRD.ORG										
Carcinogenicity (Yes/No)	0.6917 No	0.9700 No	0.6700 No	0.8800 No	0.9700 No	0.9710 No	0.7454 No	0.8100 No	0.8400 No	0.9800 No
Absorption and distribution										
	C11	C12	C13	C14	C15	C16	C17	C18	C19	C20
BBB(±)	-0.7500	-0.6750	-0.6750	-0.5750	-0.5250	-0.5500	-0.5500	+0.6250	-0.5750	+0.7000
HIA +	+0.9972	+1.0000	-0.7857	+0.7000	-0.7075	+0.7503	+0.9973	-0.7286	+0.8565	+0.9969
Aqueous Solubility(LogS)	-4.388	-3.993	-3.101	-2.457	0.447	-2.847	-1.875	-1.999	-2.457	-3.552
Metabolism										
CYP450C19 Inhibitor	0.9025 Non-inhibitor	0.5853 Non-inhibitor	0.9041 Non-inhibitor	0.9069 Non-inhibitor	0.9396 Non-inhibitor	0.9116 Non-inhibitor	0.6187 Non-Inhibitor	0.5847 Inhibitor	0.9069 Non-inhibitor	0.8244 Non-inhibitor
CYP450 1A2 Inhibitor	0.9169 Non-inhibitor	0.8153 Non-inhibitor	0.9046 Non-inhibitor	0.9045 Non-inhibitor	0.9336 Non-inhibitor	0.7872 Non-Inhibitor	0.5464 Non-Inhibitor	0.8715 Inhibitor	0.9045 Non-inhibitor	0.5339 Non-inhibitor
CYP450 3A4 Inhibitor	0.8695 Non-inhibitor	0.8144 Non-inhibitor	0.8309 Non-inhibitor	0.8744 Non-inhibitor	0.8735 Non-inhibitor	0.8646 Non-Inhibitor	0.8912 Non-Inhibitor	0.8853 Non-Inhibitor	0.8744 Non-inhibitor	0.9233 Non-inhibitor
CYP450 2C9 Inhibitor	0.9071 Non-inhibitor	0.8193 Non-inhibitor	0.9071 Non-inhibitor	0.9071 Non-inhibitor	0.9399 Non-inhibitor	0.9188 Non-inhibitor	0.9114 Non-Inhibitor	0.9167 Non-inhibitor	0.9071 Non-inhibitor	0.8269 Non-inhibitor
CYP450 2D6 Inhibitor	0.9485 Non-inhibitor	0.9457 Non-inhibitor	0.9231 Non-inhibitor	0.9388 Non-inhibitor	0.9476 Non-inhibitor	0.7293 Inhibitor	0.9505 Non-inhibitor	0.8428 Inhibitor	0.9388 Non-inhibitor	0.9632 Non-inhibitor
Excretion										
Biodegradation	0.7750 NB	0.6000 NB	0.8000 NB	0.7750 NB	0.9000 B	0.9750 NB	0.5500 NB	0.8500 NB	0.7250 NB	0.7750 NB
Toxicity										
AMES Mutagenesis	0.9000 Non-Ames toxic	0.8400 Non-Ames toxic	0.6000 Non-Ames toxic	0.9000 Non-Ames toxic	0.8800 Non-Ames toxic	0.6800 Non-Ames toxic	0.8500 Non-Ames toxic	0.7854 Non-Ames toxic	0.9000 Non-Ames toxic	0.7800 Non-Ames toxic
Acute Oral Toxicity	0.8316 III	0.8427 III	0.6433 IV	0.7775 III	0.8407 III	0.7557 III	0.7861 III	0.4795 III	0.7775 III	0.9222 III
Eye irritation (YES/NO)	No	Yes	Yes	No	Yes	No	Yes	No	No	Yes
Eye corrosion (YES/NO)	No	No	No	No	No	No	Yes	No	No	No
hERG inhibition	0.4928 No	0.7284 No	0.4678 No	0.5420 No	0.7696 No	0.6219 No	0.7194 No	0.6170 No	0.5137 No	0.7050 No
Hepatotoxicity	0.5916 Yes	0.5025 Yes	0.7375 No	0.8750 Yes	0.7875 Yes	0.5125 No	0.5197 Yes	0.6250 No	0.6125 Yes	0.5269 No
Carcinogenicity (Yes/No)	0.9900 No	0.9700 No	0.9700 No	0.9064 No	0.8030 No	1.9400 No	0.7575 No	0.9800 No	0.9064 No	0.8100 No
Absorption and distribution										
	C21	C22	C23	C24	C25	C26	C27	C28	C29	C30
BBB(±)	-0.5250	-0.5000	+0.8500	-0.8000	-0.8500	-0.5250	-0.7750	-0.8500	+0.5000	+0.9129
HIA +	+0.9316	+0.9967	+0.9936	+0.9941	-0.4855	-0.6158	-0.5116	+0.5564	+0.9970	+0.9973
Aqueous Solubility(LogS)	-2.672	-3.086	-3.502	-1.348	-2.318	-2.736	-2.449	-2.772	-4.414	-2.527
Metabolism										
CYP450C19 Inhibitor	0.8849 Non-Inhibitor	0.7660 Non-inhibitor	0.9578 Non-inhibitor	0.9651 Non-Inhibitor	0.9173 Non-inhibitor	0.8948 Non-inhibitor	0.9289 Non-inhibitor	0.9025 Non-inhibitor	0.7320 Non-inhibitor	0.5908 Non-inhibitor

© 2024 IJNRD Volume 9, Issue 7 July 2024 ISSN: 2456-4184 IJNRD.ORG										
CYP450 1A2 Inhibitor	0.8691 Non-Inhibitor	0.6580 Non-inhibitor	0.8326 Inhibitor	0.9752 Non-Inhibitor	0.9045 Non-inhibitor	0.6780 Non-inhibitor	0.9084 Non-inhibitor	0.8673 Non-inhibitor	0.8619 Non-inhibitor	0.5855 Inhibitor
CYP450 3A4 Inhibitor	0.9109 Non-Inhibitor	0.7483 Non-inhibitor	0.9484 Non-inhibitor	0.9493 Non-Inhibitor	0.9108 Non-inhibitor	0.8912 Non-inhibitor	0.9193 Non-inhibitor	0.9249 Non-inhibitor	0.8441 Non-inhibitor	0.7353 Non-inhibitor
CYP450 2C9 Inhibitor	0.9219 Non-Inhibitor	0.8175 Non-inhibitor	0.8808 Non-inhibitor	0.9697 Non-Inhibitor	0.9071 Non-inhibitor	0.9122 Non-inhibitor	0.9296 Non-inhibitor	0.9071 Non-inhibitor	0.8200 Non-inhibitor	0.6907 Non-inhibitor
CYP450 2D6 Inhibitor	0.9442 Non-inhibitor	0.9381 Non-inhibitor	0.9554 Non-inhibitor	0.9827 Non-inhibitor	0.9514 Non-inhibitor	0.6800 Non-inhibitor	0.9513 Non-inhibitor	0.9545 Non-inhibitor	0.9506 Non-inhibitor	0.6576 Inhibitor 0.9041
Excretion										
Biodegradation	0.7000 NB	0.7250 B	0.9500 B	0.9750 B	0.7250 NB	0.9750 NB	0.6750 NB	0.7500 NB	0.7750 NB	0.7750 NB
Toxicity										
AMES Mutagenesis	0.8300 Non-Ames toxic	0.8600 Non-Ames toxic	1.0000 Non-Ames toxic	1.0000 Non-Ames toxic	0.5728 Non-Ames toxic	0.6800 Non-Ames toxic	0.7000 Ames toxic	0.5400 Ames toxic	0.7100 Non-Ames toxic	0.6100 Non-Ames toxic
Acute Oral Toxicity	0.7458 III	0.7167 III	0.6378 IV	0.5472 III	0.6624 III	0.7143 III	0.4045 III	0.5971 III	0.8578 III	0.5836 III
Eye irritation (YES/NO)	No	Yes	Yes	Yes	No	No	No	No	No	No
Eye corrosion (YES/NO)	No	No	Yes	Yes	No	No	No	No	No	No
hERG inhibition	0.3669 No	0.5394 No	0.4320 No	0.9364 No	0.5971 No	0.6374 No	0.5892 No	0.4086 No	0.3607 No	0.6406 No
Hepatotoxicity	0.6375 Yes	0.7104 Yes	0.7625 Yes	0.6000 No	0.6000 No	0.5126 Yes	0.6071 No	0.5000 No	0.9250 No	0.5326 Yes
Carcinogenicity (Yes/No)	0.8664 No	0.8928 No	0.7035 No	0.6078 No	1.0000 No	0.9400 No	1.0000 No	1.0000 No	0.9200 No	0.9200 No
Absorption and distribution										
	C31	C32	C33	C34	C35	C36	C37	C38	C39	C40
BBB(±)	-0.5750	+0.8500	-0.7500	+0.8250	-0.6000	+0.8500	-0.7750	+0.8500	-0.8000	+0.6000
HIA + Aqueous Solubility(LogS)	+0.8565	+0.9936	+0.9972	+0.9947	+0.7285	+0.9654	+0.9959	+0.9936	-0.8034	+0.7285
	-2.457	-3.502	-4.388	-4.04	0.003	-2.426	-2.224	-3.502	-2.756	0.003
Metabolism										
CYP4502C19 Inhibitor	0.9069 Non-inhibitor	0.9578 Non-inhibitor	0.9025 Non-inhibitor	0.9467 Non-inhibitor	0.9170 Non-Inhibitor	0.9065 Non-inhibitor	0.9116 Non-inhibitor	0.9578 Non-inhibitor	0.8242 Non-inhibitor	0.9170 Non-inhibitor
CYP450 1A2 Inhibitor	0.9045 Non-inhibitor	0.8326 Inhibitor	0.9169 Non-inhibitor	0.9107 Inhibitor	0.8575 Non-Inhibitor	0.5259 Non-inhibitor	0.9458 Non-inhibitor	0.8326 Non-inhibitor	0.8687 Non-Inhibitor	0.8575 Non-inhibitor
CYP450 3A4 Inhibitor	0.8744 Non-inhibitor	0.9484 Non-inhibitor	0.8695 Non-inhibitor	0.9295 Non-inhibitor	0.9276 Non-Inhibitor	0.8529 Non-inhibitor	0.8693 Non-inhibitor	0.9484 Non-inhibitor	0.9289 Non-inhibitor	0.9276 Non-inhibitor
CYP450 2C9 Inhibitor	0.9071 Non-inhibitor	0.8808 Non-inhibitor	0.9071 Non-inhibitor	0.8972 Non-inhibitor	0.9064 Non-Inhibitor	0.8219 Non-inhibitor	0.9364 Non-inhibitor	0.8808 Non-inhibitor	0.8786 Non-Inhibitor	0.9064 Non-inhibitor
CYP450 2D6 Inhibitor	0.9388 Non-inhibitor	0.9554 Non-inhibitor	0.9485 Non-inhibitor	0.9545 Non-inhibitor	0.9480 Non-inhibitor	0.6480 Non-inhibitor	0.9766 Non-inhibitor	0.9554 Non-inhibitor	0.8823 Non-inhibitor	0.9480 Non-inhibitor
Excretion										
Biodegradation	0.7750 NB	0.9750 B	0.8750 NB	0.9750 B	0.5500 B	0.9000 NB	0.6000 B	1.0000 B	0.7500 NB	0.5500 B
Toxicity										

© 2024 IJNRD Volume 9, Issue 7 July 2024 ISSN: 2456-4184 IJNRD.ORG										
AMES	0.9000	1.0000	0.9600	0.9900	0.8600	0.6200	0.9700	1.0000	0.5791	0.8600
Mutagenesis	Non-Ames toxic	Non-Ames toxic	Non-Ames toxic	Non-Ames toxic	Non-Ames toxic	Non-Ames toxic	Non-Ames toxic	Non-Ames toxic	Non-Ames toxic	Non-Ames toxic
Acute Oral Toxicity	0.7775	0.6378	0.8316	0.8289	0.6755	0.7156	0.4898	0.6378	0.6716	0.6755
Eye irritation (YES/NO)	III	IV	III	IV	III	III	III	IV	III	III
Eye corrosion (YES/NO)	No	Yes	No	Yes	No	No	Yes	Yes	No	No
hERG inhibition	0.5420	0.4645	0.5287	0.3944	0.6803	0.3848	0.8830	0.5356	0.3648	0.6803
	No	No	No	No	No	No	No	No	No	No
Hepatotoxicity	0.8750	0.7625	0.8125	0.7625	0.8000	0.5572	0.7378	0.7625	0.7375	0.8000
	Yes	Yes	No	No	No	No	No	Yes	No	No
Carcinogenicity (Yes/No)	0.9064	0.7035	0.9900	0.7035	0.8023	0.9300	0.6105	0.7035	0.9900	0.8023
	No	No	No	No	No	No	No	No	No	No
Absorption and distribution										
	C41	C42	C43	C44	C45	C46	C47	C48	C49	C50
BBB(±)	-0.5750	-0.7750	-0.7750	+0.5250	-0.8500	-0.8000	+0.8500	-0.7500	-0.5250	+0.8000
HIA + Aqueous Solubility (LogS)	+0.6295	-0.5116	-0.5116	+0.6293	-0.8479	+0.9730	+0.9936	+0.9972	+1.0000	+0.9948
	-2.918	-2.449	-2.449	-0.39	-0.912	-3.306	-3.502	-4.388	-4.327	-3.618
Metabolism										
CYP450 2C19 Inhibitor	0.9044	0.9289	0.9289	0.9593	0.8671	0.7862	0.9578	0.9025N	0.7942	0.6454
	Non-inhibitor	Non-inhibitor	Non-inhibitor	Non-inhibitor	Non-inhibitor	Non-inhibitor	Non-inhibitor	on-inhibitor	Non-inhibitor	Inhibitor
CYP450 1A2 Inhibitor	0.6441	0.9084	0.9084	0.9757	0.9288	0.9106	0.8326	0.9169	0.8994	0.7828
	Non-inhibitor	Non-inhibitor	Non-inhibitor	Non-inhibitor	Non-inhibitor	Non-inhibitor	Inhibitor	Non-inhibitor	Non-inhibitor	Non-inhibitor
CYP450 3A4 Inhibitor	0.8617	0.9193	0.9193	0.9509	0.9171	0.7933	0.9494	0.8695N	0.8282	0.7681
	Non-inhibitor	Non-inhibitor	Non-inhibitor	Non-inhibitor	Non-inhibitor	Non-inhibitor	Non-inhibitor	on-inhibitor	Non-inhibitor	Non-inhibitor
CYP450 2C9 Inhibitor	0.9019	0.9296	0.9296	0.9665	0.8562	0.9071	0.8808	0.9071	0.8688	0.6312
	Non-inhibitor	Non-inhibitor	Non-inhibitor	Non-inhibitor	Non-inhibitor	Non-inhibitor	Non-inhibitor	Non-inhibitor	Non-inhibitor	Non-inhibitor
CYP450 2D6 Inhibitor	0.7223	0.9513	0.9513	0.9623	0.9206	0.9230	0.9554	0.9485	0.9397	0.9193
	Inhibitor	Non-inhibitor	Non-inhibitor	Non-inhibitor	Non-inhibitor	Non-inhibitor	Non-inhibitor	Non-inhibitor	Non-inhibitor	Non-inhibitor
Excretion										
Biodegradation	0.9750	0.7000	0.7000	0.7000	0.7250	0.5000	1.0000	0.7750	0.7250	0.5750
	NB	NB	NB	B	NB	NB	B	NB	NB	B
Toxicity										
AMES	0.6600	0.7200	0.7200	0.9400	0.6400	0.6800	1.0000	0.9000	0.8200	0.9000
Mutagenesis	Non-Ames toxic	Ames toxic	Ames toxic	Non-Ames toxic	Ames toxic	Non-Ames toxic	Non-Ames toxic	Ames toxic	Non-Ames toxic	Non-Ames toxic
Acute Oral Toxicity	0.6962	0.4045	0.4045	0.7314	0.6179	0.8059	0.6378	0.8316	0.7117	0.6521
Eye irritation (YES/NO)	III	III	III	III	III	III	IV	III	III	III
Eye corrosion (YES/NO)	No	No	No	No	No	No	Yes	No	No	Yes
hERG inhibition	No	No	No	No	No	No	Yes	No	No	No
	0.5492	0.5000	0.5000	0.7736	0.7128	0.7763	0.5479	0.4928	0.7596	0.6331
	No	No	No	No	No	No	No	No	No	No
Hepatotoxicity	0.5375	0.5196	0.5196	0.5073	0.8424	0.8875	0.7625	0.5916	0.5250	0.5928
	Yes	No	No	Yes	No	No	Yes	Yes	No	Yes
Carcinogenicity (Yes/No)	0.9400	1.0000	1.0000	0.9400	0.9600	0.9900	0.7035	0.9900	0.9700	0.8300
	No	No	No	No	No	No	No	No	No	No

Table 2b ADMET profiling of the standard drugs

Absorption and distribution							
	S1	S2	S3	S4	S5	S6	S7
BBB(±)	+0.7690	+0.9750	+0.7750	+0.625	+0.8250	+0.9000	+0.8750
HIA +	+0.9950	-0.9961	+0.9835	+0.9666	+0.9940	+0.9753	+0.8019
Aqueous Solubility (LogS)	-3.175	-3.006	-2.825	-1.774	-3.766	-0.257	-2.297
Metabolism							
CYP450 2C19	0.6653	0.5205	0.8594	0.8201	0.7415	0.9629	0.9026
Inhibitor	Inhibitor	Non-inhibitor	Non-inhibitor	Non-inhibitor	Non-inhibitor	Non-inhibitor	Non-inhibitor
CYP450 1A2	0.6313	0.8859	0.6110	0.8084	0.7089	0.9385	0.9259
Inhibitor	Inhibitor	Inhibitor	Non-inhibitor	Non-inhibitor	Non-inhibitor	Non-inhibitor	Non-inhibitor
CYP450 3A4	0.7468	0.5219	0.7678	0.8370	0.8621	0.9352	0.9037
Inhibitor	Non-inhibitor	Non-inhibitor	Non-inhibitor	Non-inhibitor	Non-inhibitor	Non-inhibitor	Non-inhibitor
CYP450 2C9	0.7071	0.8616	0.9071	0.8704	0.7991	0.9425	0.9071
Inhibitor	Non-inhibitor	Non-inhibitor	Non-inhibitor	Non-inhibitor	Non-inhibitor	Non-inhibitor	Non-inhibitor
CYP450 2D6	0.8770	0.253	0.7007	0.8775	0.9064	0.9539	0.9625
Inhibitor	Inhibitor	Non-inhibitor	Inhibitor	Non-inhibitor	Non-inhibitor	Non-inhibitor	Non-inhibitor
Excretion							
Biodegradation	0.8000 NB	0.8250 NB	0.9250 NB	0.7250 NB	0.7500 NB	0.6250 B	0.7000 NB
Toxicity							
AMES	0.6901	0.7300	0.5400	0.5000	0.6600	0.8755	0.5700
Mutagenesis	Non-Ames toxic	Non-Ames toxic	Ames toxic	Non-Ames toxic	Non-Ames toxic	Non-Ames toxic	Non-Ames toxic
Acute Oral Toxicity	0.6321 III	0.7268 II	0.6525 II	0.7619 III	0.6679 III	0.5319 III	0.6485 III
Eye irritation (YES/NO)	No	No	No	No	No	Yes	No
Eye corrosion (YES/NO)	No	No	No	No	No	Yes	No
hERG inhibition	0.4871 No	0.7259 No	0.7260 No	0.3720 No	0.7584 No	0.7695 No	0.6570 No
Hepatotoxicity	0.6750 Yes	0.8000 Yes	0.6375 Yes	0.7966 No	0.7605 Yes	0.8750 Yes	0.9125 Yes
Carcinogenicity (Yes/No)	0.6538 No	1.6400 No	0.7919 No	0.7700 No	0.8400 No	0.5815 Yes	0.6713 No

C1- 2-hydroxyacetophenone, **C2-** 6 α -carissanol, **C3-13**-heptadecyn-1-ol, **C4-** 20-hydroxypregnan-18-oic acid, **C5** –Berberine, **C6**-bisorargemonine, **C7**-caffeic acid methyl ester, **C8**-carandinol, **C9**-Carenone, **C10**-carindone, **C11**-Carissic acid, **C12**-Carisone, **C13**-catechin, **C14**-Chlorogenic acid, **C15**- Citric acid, **C16**-columbamine, **C17**-Coniferaldehyde, **C18**-coreximine, **C19**-Cryptovhlorogenic acid, **C20**-cryptomeridiol, **C21**-Dicaffeoylquinic acid, **C22**-Germacrenone, **C23**-Heptadecanoic acid, **C24**-hydroxybenzoic acid, **C25**-isorhamnetin-3-O-beta-d-glucopyranoside, **C26**-Jateorrhizine, **C27**- kaempferol-3-O-beta-d-glucopyranoside, **C28**- kaempferol-3-O-robinobioside, **C29**-lupeol, **C30**-Morphinandione, **C31**-Neochlorogenic acid, **C32**- n-hexadecanoic acid, **C33**-oleanolic acid, **C34**- oleic acid, **C35**-ononitol, **C36**-pallidine, **C37**- p-coumaric acid, **C38**-pentadecanoic acid, **C39**-Peonidin 3-rutinoside, **C40**-pinitol, **C41**-Psuedocolumbamine, **C42**- quercetin-3-O-glucoside, **C43**- quercetin-3-O-beta-d-glucopyranoside, **C44**-Quinic acid, **C45**-salicin, **C46**-scopoletin, **C47**-Tetradecanoic acid, **C48**-Ursolic acid, **C49**- alpha-carissanol, **C50**- β -eudesmol, **S1**-Cenobamate, **S2**-Fenfluramine, **S3**- Lamotrigine, **S4**-Lacosamide, **S5**-Eslicarbazepine, **S6**-Pregabalin, **S7**- Acetazolamide.

The results of the ADMET analysis revealed that, out of 99 compounds tested, only 50 compounds (C1-C50) passed the ADMET analysis (Table 2a), with others having severe acute toxicity and hERG inhibition issues, among other important factors considered during the screening process. As observed in Tables 2a and 2b, the selected compounds (C1- C50) and the standards (S1 to S7) have positive intestine absorption (HIA+) except C3, C6, C10, C13, C15, C25, C26, C27, C39, C42, C43, C45, and S2, thus can easily be absorbed in the intestine of human. Compounds (C1, C3, C4, C5, C6, C8, C9, C10, C14, C18, C20, C23, C29, C30, C32, C34, C36, C38, C40, C44, C45, C47, and C50) and the standard (S1-S7) possess the ability to cross the blood-brain barrier (BBB+) while all the selected compounds (C1-50) and standards (S1-S7) aqueous solubility (log S) values are within -1 to -5 recommended range for compounds with acceptable solubility value (Tsaion and Kates, 2011), thus, the selected compound and standards have reliable absorption and distribution properties.

Cytochrome (P450 inhibitors), i.e. the microsomal enzymes responsible for the catalytic reactions involved in drug metabolic activities were used to evaluate the metabolic activities of the selected compounds

and standards. An excellent drug candidate is expected to be non-inhibitors of these enzymes except in rare cases. Furthermore, except for a few enzymes, the selected compounds and standards are non-inhibitors of the cytochrome (P450) inhibitors. As expected, the selected compounds are non-carcinogenic and non-ame toxic. Compounds (C7, C13, C23, C32, 34, C38, and C47) possess Type IV acute oral toxicity profile (i.e. non-toxic), while others have acceptable toxicity Type III (slightly toxic) which could easily be modified to Type IV (non-toxic) (Onawole et al. 2017, Abdul-Hammed et al. 2021). However, the toxicity profile of the selected compounds is far better than most of the commercial drugs used as standards especially the acute oral toxicity profile of S2 (Fenfluramine) and S3 (Lamotrigine) with Type II acute oral toxicity profile. Moreover, all the selected compounds and standards are non-inhibitors of Human ether-a-go-go (hERG2), an important property to be considered in drug discovery and development whose inhibition can block the potassium ion channel of the myocardium, thereby resulting in heart or cardiac arrest which may lead to death (Sanguinetti and Tristani-firouzi 2006; Abdul-Hammed et al. 2021).

Moreover, a close examination of Table 2a and 2b revealed that some compounds and standards despite their excellent ADMET properties are hepatotoxic; thus, they are discarded for further analysis except S7 (acetazolamide (AZM), a native inhibitor and co-factor located and interacted with the active site of all target receptors used in this study. Summarily, compounds (C3, C4, C6, C7, C8, C10, C13, C16, C18, C20, C24, C25, C27, C28, C29, C33, C34, C35, C36, C37, C38, C40, C42, C43, C45, C46, C49, S4, and S7 show outstanding ADMET properties, and this, reliable and safe to be tested further as potential inhibitors of the CA target receptors.

3.3 Drug-likeness Analysis of the selected compounds

One of the pivotal operations in the early stage of the drug discovery process is an analysis of the drug-likeness potential of the probable drug molecules. This could be achieved using the Lipinski filter as established by the rule of five (RO5) (Lipinski, 2004). The rule states that for a molecule should be considered an oral drug, it must possess molecular weight (MW) $\leq 500\text{gmol}^{-1}$, hydrogen bond donor (HBD's) ≤ 5 , hydrogen bond acceptor (HBA's) ≤ 10 , and Octanol Water Partition Co-efficient (Log P) ≤ 5 with only one (1) violation accepted. For the current investigation, 27 compounds and 2 standards from ADMET screening were subjected to drug-likeness analysis as shown in Table 3. However, after the thorough screening, only 22 compounds passed the RO5 test with no or one violation as reported in Table 3 and the successful compounds will be subjected to further analysis while others will be discarded.

Table 3 Drug Likeness properties of the best hits and the standard drug (S4 and S7)

Compound s	Molecular Formula	Heavy atoms (HA)	Molecular weight	RO5 violation (n5)	Hydrogen bond donor (HBD)	Hydrogen acceptor (HBA)	ALog P
C3	C ₁₇ H ₃₂ O	18	252.44	1	1	1	5.07
C4	C ₂₁ H ₃₄ O ₃	24	334.49	0	2	3	4.48
C6	C ₁₉ H ₂₁ NO ₄	24	327.37	0	2	5	2.94
C7	C ₁₀ H ₁₀ O ₄	14	194.18	0	2	4	1.28
C8	C ₃₀ H ₅₂ O ₂	32	444.73	1	2	2	7.22
C10	C ₃₁ H ₄₄ O ₆	37	512.68	1	2	6	4.65
C13	C ₁₅ H ₁₄ O ₆	21	290.27	0	5	6	1.55
C16	C ₂₀ H ₂₀ NO ₄ ⁺	25	338.38	0	1	4	3.08
C18	C ₁₉ H ₂₁ NO ₄	24	327.37	0	2	5	2.77
C20	C ₁₅ H ₂₈ O ₂	17	240.38	0	2	2	3.11
C24	C ₇ H ₆ O ₃	10	138.12	0	2	3	1.09
C29	C ₃₀ H ₅₀ O	31	426.72	1	1	1	8.02
C33	C ₃₀ H ₄₈ O ₃	33	456.7	1	2	3	7.33
C34	C ₁₈ H ₃₄ O ₂	20	282.46	1	1	2	6.11
C35	C ₇ H ₁₄ O ₆	13	194.18	0	5	6	-3.18
C36	C ₁₉ H ₂₁ NO ₄	24	327.37	0	1	5	1.94
C37	C ₉ H ₈ O ₃	12	164.16	0	2	3	1.49
C38	C ₁₅ H ₃₀ O ₂	17	242.4	0	1	2	5.16
C40	C ₇ H ₁₄ O ₆	13	194.18	0	5	6	-3.18
C45	C ₁₃ H ₁₈ O ₇	20	286.28	0	5	7	-1.64
C46	C ₁₀ H ₈ O ₄	14	192.17	0	1	4	1.51

C49	C₁₅H₂₄O₃	18	252.35	0	2	3	2.21
S4	C₁₃H₁₈N₂O₃	18	250.29	0	2	3	0.45
S7	C₄H₆N₄O₃S₂	13	222.25	0	2	6	-0.86

C3-13-heptadecyn-1-ol, **C4**-20-hydroxypregnan-18-oic acid, **C6**-bisorargemonine, **C7**-caffeic acid methyl ester, **C8**-carandiol, **C10**-carindone, **C13**-catechin, **C16**-columbamine, **C18**-coreximine, **C20**-cryptomeridiol, **C24**-hydroxybenzoic acid, **C29**-lupeol, **C33**-oleanolic acid, **C34**-oleic acid, **C35**-ononitol, **C36**-pallidine, **C37**-p-coumaric acid, **C38**-pentadecanoic acid, **C40**-pinitol, **C45**-salicin, **C46**-scopoletin, **C49**-alpha-carissanol, **S4**-Lacosamide, **S7**-Acetazolamide

3.4 Protein-Ligand Molecular Docking Analysis

The molecular docking technique is the most widely adopted and reliable method of investigating the potency of a compound against a target protein (Abdul-Hammed et al. 2021; Oyebamiji et al., 2023; William et al., 2024). It gives the binding energies from which the inhibitory efficiency of a probable drug candidate can be determined. In this study, twenty-two (22) compounds with excellent drug-likeness profiles and two (2) standards were docked against two well-validated anti-epilepsy drug targets (*Human carbonic anhydrase VII and XIV with (PDB ID: 3ML5), and (PDB ID: 4LU3)* respectively in triplicate using PyRx-docking software. The Mean and Standard Deviation (SD) of the docking scores (binding affinity ΔG (kcal/mol)) were evaluated, while the Inhibition constant (K_i) in μM was calculated. Table 4 shows the result of the docking simulation.

A close examination of Table 4 shows the interactions of the docked compounds with the CA VII (PDB: 3ML5) and CA XIV (PDB ID: 4LU3) target receptors respectively. It was observed that the binding affinities of the docked compounds range from -8.1 kcal/mol to -5.1 kcal/mol for 3ML5, and -8.0 kcal/mol to -5.3 kcal/mol for 4LU3 with C4 (-8.1 kcal/mol) and C33 (-8.0 kcal/mol) having the highest binding affinities in each set, respectively. As observed in the 3HS4 docking result, several docked compounds have better binding affinities against 3ML5 and 4LU3 receptors than the standards (S4, -6.9 kcal/mol, and S7, -6.4 kcal/mol) for 3ML5 and (S4, -6.7kcal/mol and S7, -6.4 kcal/mol) for 4LU3. The (K_i) values of these compounds are also lower than that of the standards which indicate their better inhibitory efficiency against 3ML5 and 4LU3 targets as compared to S4 and S7. Summarily, compounds (C4, C8, C6, C18, C33, C13, C29, C36, C45, C10, and C16) are better inhibitors of 3ML5 than S4 and S7, while C33, C10, C29, C13, C8, C18, C36, C4, C49, C6, C16, C45 and C20 have better binding affinities in the active site of 4LU3 than S4 and S, and could be subjected to further screening towards the discovery of novel anti-epilepsy therapy.

Table 4 Docking scoring and the inhibition constants of selected phytochemicals with Carbonic anhydrase, CA VII target receptor (PDB ID: 3ML5) and Carbonic anhydrase, CA XIV target receptor (PDB ID: 4LU3).

CA VII target receptor (PDB ID: 3ML5)				CA XIV target receptor (PDB ID: 4LU3).			
S/N	Ligands	Binding Affinity (ΔG), kcal/mol	Inhibition Constant (K_i), μM	S/N	Ligands	Binding Affinity (ΔG), kcal/mol	Inhibition Constant (K_i), μm
1.	C4	-8.1 \pm 0.10	1.16	1.	C33	-8.0 \pm 0.10	1.39
2.	C8	-8.1 \pm 0.00	1.16	2.	C10	-7.8 \pm 0.10	1.94
3.	C6	-7.7 \pm 0.00	2.28	3.	C29	-7.8 \pm 0.00	1.94
4.	C18	-7.7 \pm 0.10	2.28	4.	C13	-7.8 \pm 0.00	1.94
5.	C33	-7.6 \pm 0.00	2.7	5.	C8	-7.6 \pm 0.00	2.70
6.	C13	-7.5 \pm 0.00	3.23	6.	C18	-7.6 \pm 0.00	2.70
7.	C29	-7.5 \pm 0.00	3.23	7.	C36	-7.6 \pm 0.00	2.70
8.	C36	-7.3 \pm 0.00	4.48	8.	C4	-7.5 \pm 0.10	3.20
9.	C45	-7.3 \pm 0.00	4.48	9.	C49	-7.5 \pm 0.00	3.20
10.	C10	-7.2 \pm 0.00	5.30	10.	C6	-7.4 \pm 0.00	3.83
11.	C16	-7.2 \pm 0.00	5.30	11.	C16	-7.4 \pm 0.10	3.83
12.	S4	-6.9 \pm 0.20	8.80	12.	C45	-7.3 \pm 0.00	4.48
13.	C49	-6.9 \pm 0.00	8.80	13.	C20	-6.7 \pm 0.00	12.33
14.	C46	-6.5 \pm 0.00	17.27	14.	S4	-6.7 \pm 0.00	12.33
15.	C7	-6.4 \pm 0.00	20.45	15.	C7	-6.6 \pm 0.00	14.59
16.	C20	-6.4 \pm 0.10	20.45	16.	C46	-6.5 \pm 0.00	17.27
17.	S7	-6.4 \pm 0.00	20.45	17.	S7	-6.4 \pm 0.10	20.45
18.	C37	-5.9 \pm 0.10	47.53	18.	C37	-6.0 \pm 0.00	40.51
19.	C40	-5.6 \pm 0.00	78.85	19.	C24	-5.8 \pm 0.10	56.75
20.	C38	-5.5 \pm 0.20	93.34	20.	C34	-5.8 \pm 0.00	56.75
21.	C24	-5.4 \pm 0.10	110.50	21.	C40	-5.7 \pm 0.00	69.16
22.	C34	-5.4 \pm 0.00	110.50	22.	C38	-5.5 \pm 0.10	93.34
23.	C35	-5.3 \pm 0.10	130.80	23.	C35	-5.4 \pm 0.10	110.50

24.	C3	-5.1 ± 0.10	183.30	24.	C3	-5.3 ± 0.10	130.80
-----	----	-------------	--------	-----	----	-------------	--------

** The binding affinity values are the mean and Standard deviation (Mean ± SD) of three determinations.

C3-13-heptadecyn-1-ol, **C4**-20-hydroxypregnan-18-oic acid, **C6**- Bisorargemonine, **C7**- Caffeic acid methyl ester, **C8**-Carandinol, **C10**-Carindone, **C13**-Catechin, **C16**-Columbamine, **C18**-Coreximine, **C20**-Cryptomeridiol, **C24**-Hydroxybenzoic acid, **C29**-Lupeol, **C33**-Oleanolic acid, **C34**- oleic acid, **C35**-Ononitol, **C36**- Pallidine, **C37**- p-Coumaric acid, **C38**-Pentadecanoic acid, **C40**-pinitol, **C45**-Salicin. **C46**-Scopoletin, **C49**- alpha-carissanol, **S4**-Lacosamide, **S7**- Acetazolamide

3.5 Oral-bioavailability studies of the selected hit compounds

SwissADME tool (<http://www.swissadme.ch/>) was used to investigate the oral bioavailability properties of the selected compounds (Daina et al. 2017). The bioavailability RADAR (Fig. 3) shows the oral bioavailability profile of the hit and standards at a glance with the pink area in the RADAR showing the most favourable zone for each of the bioavailability properties. As observed in Table 5, all the selected hits and standards except C10 obeyed the 500 g/mol recommended (SIZE) for bioavailable compounds as opined by Lipinski's rule of five. The polarity (POLAR) of the selected hit and standards were examined using Total Polarity Surface Area (TPSA) whose recommended range is between 20 and 130 Å². All the selected compounds have TPSA which falls within the recommended value as compared to the standard S7 with a TPSA of 151.66. The number of rotatable bonds whose value should not exceed nine (9) was used to evaluate the flexibility (FLEX) of the selected hit and standards. Also, except for C3 (12), C34 (15), and C38 (15), the number of rotatable bonds in all the selected hits and standards falls within the recommended range. XlogP3 and ESOL (log S) are used to determine the compound lipophilicity (LIPO) and insolubility (INSOLU), and the recommended ranges for the two properties are -0.7 and +5.0 and 0 and 6, respectively. The LIPO and INSOLU of the selected hits and standard are within the recommended range except for C3, C8, C29, C33, C34, and C38 for xlogP3, and C8, C29, and C33 for ESOL. Fraction Csp3 whose recommended range is 0.5 and 1 was used to evaluate the Unsaturation (INSATU) of the selected hit. Interestingly, all the hits and standards have values within the recommended range. The hit and standards evaluated have appreciable bioavailability scores of (0.55) with higher bioavailability scores of (0.85) recorded for C33, C34, C37, C38, C24, and C4. In consequence, all the selected hit possesses reliable oral-bioavailability properties as compared to the standards.

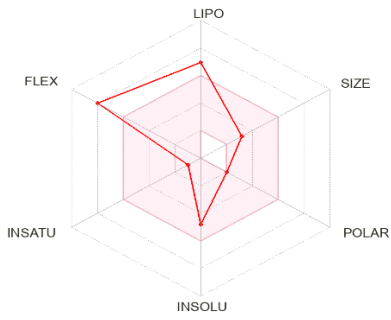
Table 5 Oral bioavailability of the selected compounds and standards

LIGAND	C3	C4	C6	C7	C8	C10
Formula	C ₁₇ H ₃₂ O	C ₂₁ H ₃₄ O ₃	C ₁₉ H ₂₁ NO ₄	C ₁₀ H ₁₀ O ₄	C ₃₀ H ₅₂ O ₂	C ₃₁ H ₄₄ O ₆
VINA Score	-4.9 (3HS4) -5.1 (3ML5) -5.3 (4LU3)	-8.1 (3HS4) -8.1 (3ML5) -7.5 (4LU3)	-7.3 (3HS4) -7.7 (3ML5) -7.4 (4LU3)	-6.7 (3HS4) -6.4 (3ML5) -6.6 (4LU3)	-7.3 (3HS4) -8.1 (3ML5) -7.6 (4LU3)	-6.8 (3HS4) -7.2 (3ML5) -7.8 (4LU3)
Mass	252.44	334.49	327.37	194.18	444.73	512.68
TPSA	20.23	57.53	62.16	66.76	40.46	100.9
#Rotatable bonds	12	2	2	3	1	2
XLOGP3	6.65	5.41	2.62	1.48	8.33	3.68
WLOGP	5.15	4.48	1.91	1.18	7.22	4.65
ESOL Log S	-4.8	-5.19	-3.76	-2.1	-7.78	-5.21
ESOL Class	Moderately soluble	Moderately soluble	Soluble	Soluble	Poorly soluble	Moderately soluble
Lipinski #violation	1	0	0	0	1	1
Bioavailability Score	0.55	0.85	0.55	0.55	0.55	0.55
PAIN #alerts	0	0	0	1	0	0
Fraction Csp3	0.88	0.95	0.37	0.10	1.00	0.77
Synthetic Accessibility	4.04	4.56	3.32	2.01	5.46	6.83

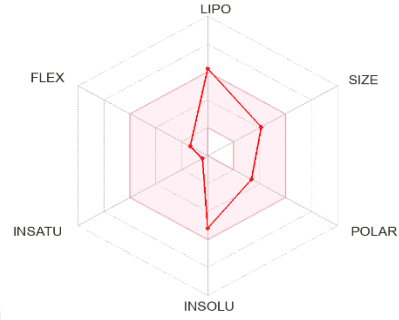
LIGAND	C13	C16	C18	C20	C24	C29
Formula	C ₁₅ H ₁₄ O ₆	C ₂₀ H ₂₀ NO ₄ ⁺	C ₁₉ H ₂₁ NO ₄	C ₁₅ H ₂₈ O ₂	C ₇ H ₆ O ₃	C ₃₀ H ₅₀ O
VINA Score	-7.4 (3HS4) -7.5 (3ML5) -7.8 (4LU3)	-8.0 (3HS4) -7.2 (3ML5) -7.4 (4LU3)	-7.5 (3HS4) -7.7 (3ML5) -7.6 (4LU3)	-6.6 (3HS4) -6.4 (3ML5) -6.7 (4LU3)	-6.0 (3HS4) -5.4 (3ML5) -5.8 (4LU3)	-7.6 (3HS4) -7.5 (3ML5) -7.8 (4LU3)
Mass	290.27	338.38	327.37	240.38	138.12	426.72

TPSA	110.38	51.8	62.16	40.46	57.53	20.23
#Rotatable bonds	1	3	2	1	1	1
XLOGP3	0.36	3.42	2.59	2.95	1.58	9.87
WLOGP	1.22	3.08	1.91	3.11	1.09	8.02
ESOL Log S	-2.22	-4.37	-3.74	-3.12	-2.07	-8.64
ESOL Class	Soluble	Moderately soluble	Soluble	Soluble	Soluble	Poorly soluble
Lipinski #violation	0	0	0	0	0	1
Bioavailability Score	0.55	0.55	0.55	0.55	0.85	0.55
PAIN #alerts	1	0	0	0	0	0
Fraction Csp3	0.2	0.25	0.37	1.00	0	0.93
Synthetic Accessibility	3.5	3.05	3.32	3.55	1.00	5.49
LIGAND	C33	C34	C35	C36	C37	C38
Formula	C ₃₀ H ₄₈ O ₃	C ₁₈ H ₃₄ O ₂	C ₇ H ₁₄ O ₆	C ₁₉ H ₂₁ NO ₄	C ₉ H ₈ O ₃	C ₁₅ H ₃₀ O ₂
VINA Score	-7.9 (3HS4) -7.6 (3ML5) -8.0 (4LU3)	-5.3 (3HS4) -5.4 (3ML5) -5.8 (4LU3)	-5.4 (3HS4) -5.3 (3ML5) -5.4 (4LU3)	-7.1 (3HS4) -7.3 (3ML5) -7.6 (4LU3)	-5.8 (3HS4) -5.9 (3ML5) -6.0 (4LU3)	-5.4 (3HS4) -5.5 (3ML5) -5.5 (4LU3)
Mass	456.7	282.46	194.18	327.37	164.16	242.40
TPSA	57.53	37.3	110.38	59.00	57.53	37.3
#Rotatable bonds	1	15	1	2	2	13
XLOGP3	7.49	7.64	-3.17	1.95	1.46	6.63
WLOGP	7.23	6.11	-3.18	1.56	1.38	5.16
ESOL Log S	-7.32	-5.41	1.02	-3.15	-2.02	-4.66
ESOL Class	Poorly soluble	Moderately soluble	Highly soluble	Soluble	Soluble	Moderately soluble
Lipinski #violation	1	1	0	0	0	0
Bioavailability Score	0.85	0.85	0.55	0.55	0.85	0.85
PAIN #alerts	0	0	0	0	0	0
Fraction Csp3	0.9	0.83	1.00	0.42	0.00	0.93
Synthetic Accessibility	6.08	3.07	3.76	4.47	1.61	2.20
LIGAND	C40	C45	C46	C49	S4	S7
Formula	C ₇ H ₁₄ O ₆	C ₁₃ H ₁₈ O ₇	C ₁₀ H ₈ O ₄	C ₁₅ H ₂₄ O ₃	C ₁₃ H ₁₈ N ₂ O ₃	C ₄ H ₆ N ₄ O ₃ S ₂
VINA Score	-5.5 (3HS4) -5.6 (3ML5) -5.7 (4LU3)	-7.4 (3HS4) -7.3 (3ML5) -7.3 (4LU3)	-6.8 (3HS4) -6.5 (3ML5) -6.5 (4LU3)	-7.6 (3HS4) -6.9 (3ML5) -7.5 (4LU3)	-7.1 (3HS4) -6.9 (3ML5) -6.7 (4LU3)	-6.4 (3HS4) -6.4 (3ML5) -6.4 (4LU3)
Mass	194.18	286.28	192.17	252.35	250.29	222.25
TPSA	110.38	119.61	59.67	57.53	67.43	151.66
#Rotatable bonds	1	4	1	1	8	3
XLOGP3	-3.17	-1.22	1.53	1.73	0.27	-0.26
WLOGP	-3.18	-1.79	1.51	2.21	0.3	0.03
ESOL Log S	1.02	-0.80	-2.46	-2.43	-1.28	-1.14
ESOL Class	Highly soluble	Very soluble	Soluble	Soluble	Very soluble	Very soluble
Lipinski #violation	0	0	0	0	0	0
Bioavailability Score	0.55	0.55	0.55	0.55	0.55	0.55
PAIN #alerts	0	0	0	0	0	0
Fraction Csp3	1.00	0.54	0.10	0.80	0.38	0.25
Synthetic Accessibility	3.76	4.23	2.62	4.13	2.27	3.00

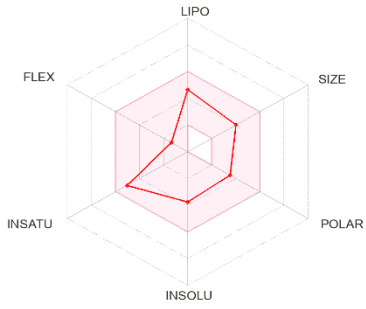
C3-13-heptadecyn-1-ol, C4-20-hydroxypregnan-18-oic acid, C6- Bisorargemonine, C7- Caffeic acid methyl ester, C8-Carandiol, C10-Carindone, C13-Catechin, C16-Columbamine, C18-Coreximine, C20-Cryptomeridiol, C24-Hydroxybenzoic acid, C29-Lupeol, C33-Oleanolic acid, C34- oleic acid, C35-Ononitol, C36-Pallidine, C37- p-Coumaric acid, C38-Pentadecanoic acid, C40-pinitol, C45-Salicin. C46-Scopoletin, C49- alpha-carissanol, S4-Lacosamide, S7- Acetazolamide



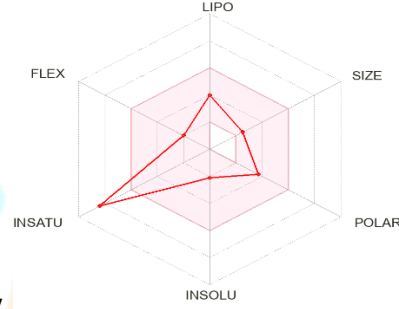
C3



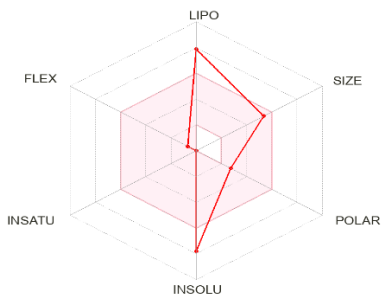
C4



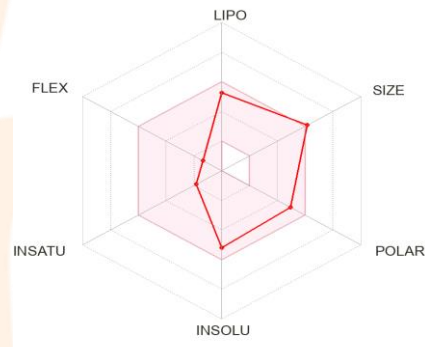
C6



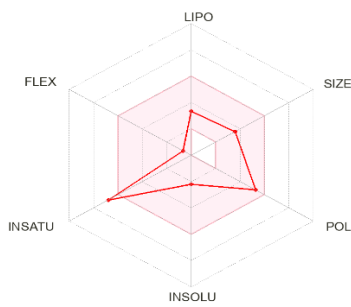
C7



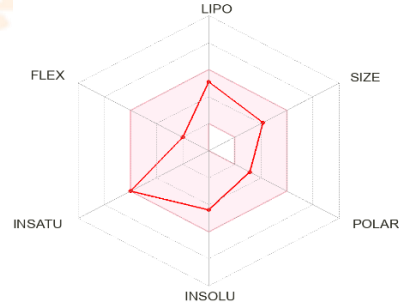
C8



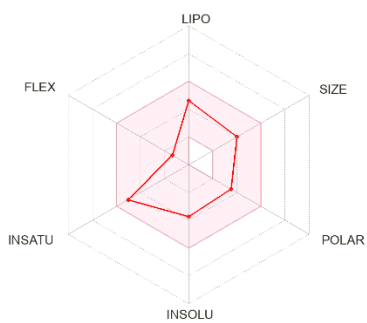
C10



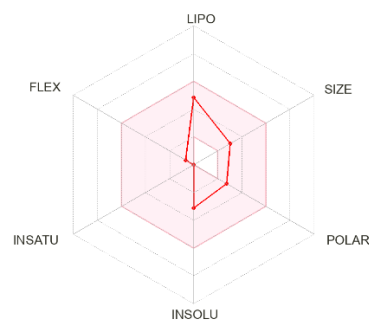
C13



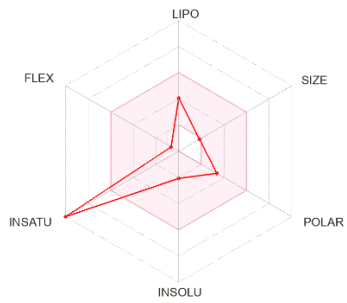
C16



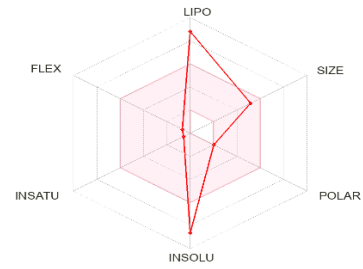
C18



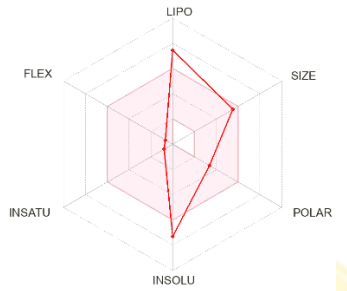
C20



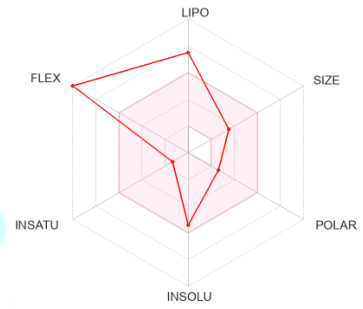
C24



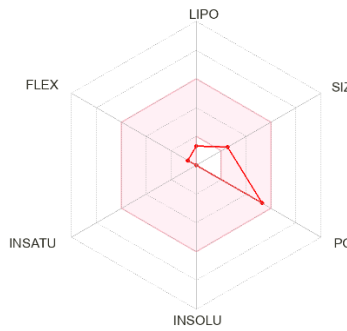
C29



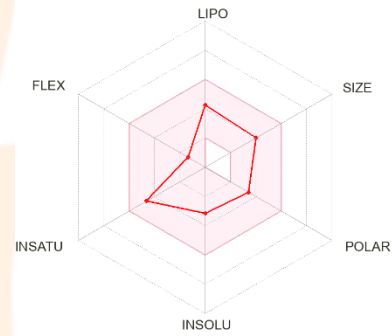
C33



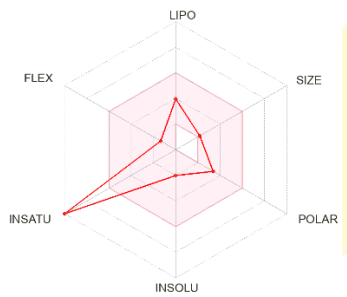
C34



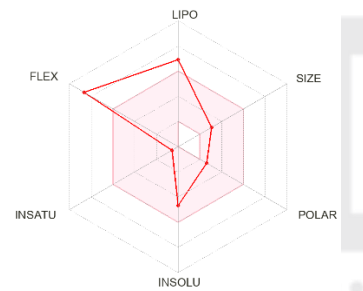
C35



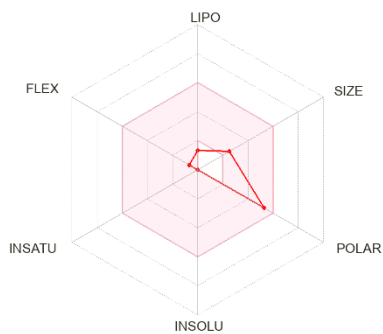
C36



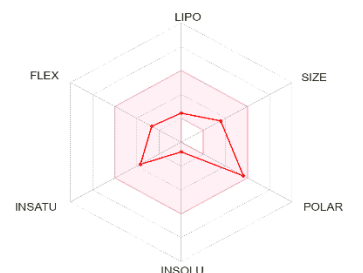
C37



C38



C40



C45

International Research Journal
IJNRD
Research Through Innovation

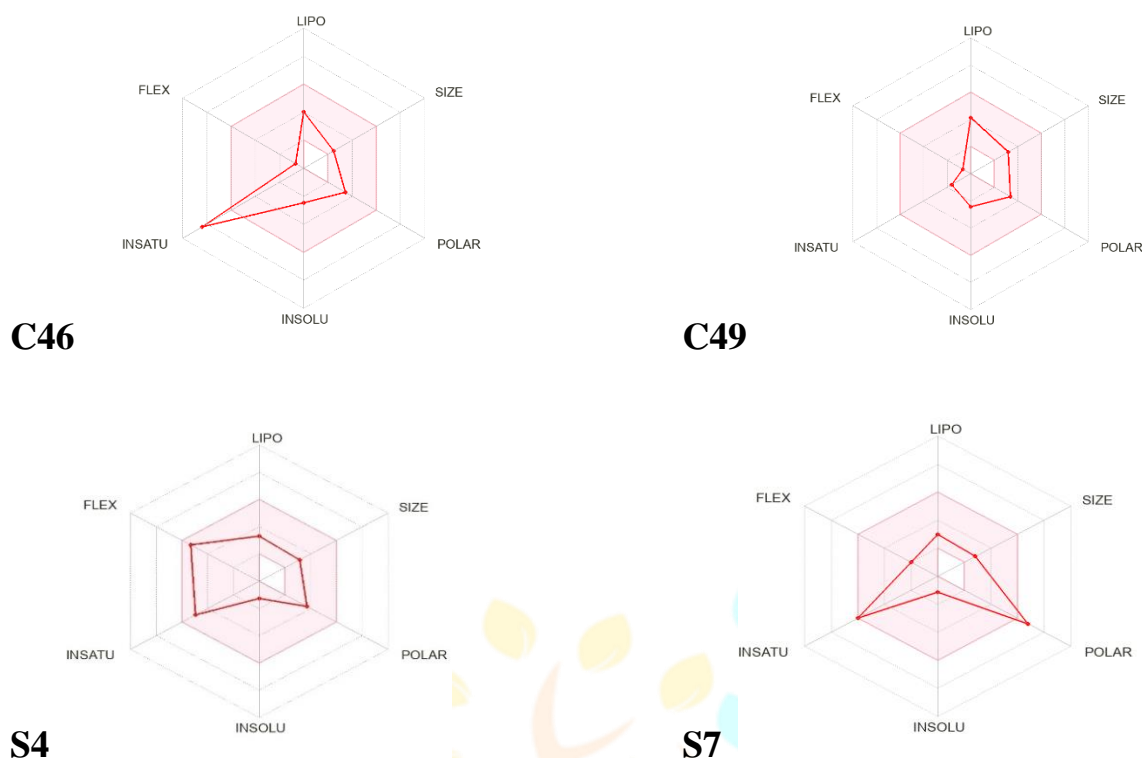


Fig 3 The bioavailability radar for the selected hit and standard

3.6 Lead-likeness Analysis of the selected compounds and standards

The lead-like property of a molecule remains an indispensable feature worthy of evaluation in a quest to design an effective drug that can reach and remain in the target site without denaturation (Daina, et al. 2017). A good lead (bioactive compound) is a molecular entity suitable for optimization i.e. lead is subjected to chemical modifications that would most likely increase size and lipophilicity (Daina et al. 2017). Therefore, leads are required to be smaller in size and less hydrophobic than drug-like molecules. As shown in Table 6, the lead-likeness profile of the 22 hit and 2 standard drugs was examined using a method implemented by Teague (1999). It states that for a molecule to be considered a lead-like molecule, it should possess $250 \leq MW \leq 350$, $XlogP \leq 3.5$, Number of rotatable bonds ≤ 7 . However, a close examination of Table 6 shows that of all the 22 ligands examined, only seven (7) compounds were able to fulfill the lead-likeness rule. Compounds C6, C13, C16, C18, C36, C45, and C49 obeyed all the lead-like rules, they possessed molecular weight (MW), Octanol water partition coefficient (XlogP) and number of rotatable bonds within the recommended range compared to the two standards with one violation each S4 = (Rotors > 7) and S7 = (MW < 250). Thus, C6, C13, C16, C18, C36, C45, and C49 are reliable lead-like compounds that could be further optimized to improve their potency and efficacy, reduce their toxicity, and improve their pharmacokinetics.

3.7 Prediction of Activity Spectra for Substances (PASS)

The probable anti-epilepsy, anti-convulsion, or anti-seizure biological activities of the selected leads and standard were examined using the reliable PASS web-server, (Goel et al. 2011). The result of the investigations as shown in Table 7 revealed that (C13, C6, C18, C45, C49, and S4) possess one or more anti-epilepsy activities with the probability of being active (P_a^a) greater than the probability of being inactive (P_i^b). This shows that the identified leads are probable anti-epilepsy agents and could be further developed.

3.8 Binding mode and molecular interactions of the identified leads with the targets

Investigating the biological activities and interactions of a potential drug molecule with the active site of the target is an important operation in novel drug discovery and development. It aids in identifying how best a ligand (lead) interacts with the required site which gives information on how to improve its potency and efficacy during the optimization stage of the drug discovery process. The current investigation explored the binding mode and molecular interactions of seven (7) lead molecules with the two standards whose binding affinity and interaction with the main active sites of the target have been established as shown in Fig. 4 and Fig. 5.

A close examination of the interactions of the selected lead with the **3ML5** receptor as shown in Fig. 4 revealed that C6 formed a conventional hydrogen bond with Thr199, His96, His94, Gln92, Pro201, and Gly1, carbon-hydrogen bond with Pro202, and

Pi-Alkyl interaction with Leu198. C13 formed conventional hydrogen bonds with Gln67, and Thr199, unfavourable Donor-Donor with Trp5, Pi-cation with His94, Pi-sigma with Leu198 and Pi-Alkyl with Val121. Pi-Pi T-shaped interaction was also observed. Moreover, Fig. 4 shows that C16 formed conventional hydrogen bonds with Thr199, and His94, and Alkyl and Pi-Alkyl interaction with Leu198. C36 formed a carbon-hydrogen bond with His94 and Pro202, as well as Pi-Alkyl interaction with His2. C45 formed a conventional hydrogen bond with Asn62, carbon-hydrogen bond with Ser65, Pi-cation with His94, Pi-Alkyl interaction with Val143 and Val121, Pi-sig a with Leu198, while Pi-Pi T-shaped was also observed. Also, the figure revealed that the two standards also show favourable interaction with the **3ML5** receptor with S4 forming a conventional hydrogen bond with Gln92, carbon hydrogen bond with Ser65, Pi-cation with His94, Pi-Alkyl with Leu198, unfavourable Donor-Donor with Thr200, and Pi-Pi T-shaped was also observed. Similarly, S7 also formed conventional hydrogen bonds with Thr199, His96, His119, His94, and Thr200, Pi-sigma interaction with Leu198, and Pi-sulfur bond with Trp209. Consequently, most of the amino residues displayed by the leads and standards are part of amino acids in the active site of the **3ML5** receptor. This indicates that the leads shared the same pocket and also interacted effectively with the active site of the target.

Similarly, Fig. 5 shows the binding mode and interactions of the selected lead with the **4LU3** target receptor. It was clearly shown that C6 formed a conventional hydrogen bond with Thr199, Pro201, and Trp5, a carbon-hydrogen bond with Pro202, Pi-Alkyl interaction with Leu198, and unfavourable Donor-Donor with His119, His96, and His94. C13 formed conventional hydrogen bonds with Trp5, and Thr199, Pi-cation interaction with His94, Pi-Alkyl interaction with Val121 and Leu198, while Pi-Pi T-shaped was also observed. C16 formed conventional hydrogen bonds with Thr200, Pi-sigma interaction with Leu198, Alkyl and Pi-Alkyl interaction with Ala135, Val121, Leu131, and Leu141. C18 formed a conventional hydrogen bond with Thr200, a carbon-hydrogen bond with Ser132, a Pi-Sigma interaction with Leu198, Alkyl and Pi-Alkyl bond with Leu141, leu131, Val121, and Ala135, and a Pi-Pi T-shaped interaction with His94. Moreover, it was observed that C36 effectively interacts with the receptor, showing conventional hydrogen bond interaction with Asn62, carbon-hydrogen bond with Gln67, Pi-Donor hydrogen bond with Thr199, and Alkyl interaction with Leu198, and Ala135. C45 formed conventional hydrogen bonds with Thr199, and Asn62, Pi-sigma interaction with Leu198, Pi-Alkyl interaction with Val121, and Pi-Pi T-shaped interaction with His94. C49 formed a conventional hydrogen bond with Gln67, and Asn62, unfavourable Donor-Donor with Thr199, Pi-Sigma with His94, and Alkyl and Pi-Alkyl interaction with Val121, Leu198, and His96. The two standard S4 and S7 also interact with the 4LU3 receptor. S4 formed a conventional hydrogen bond with Thr200, a carbon-hydrogen bond with Thr199, a Pi-sigma bond with Leu198, Pi-Alkyl bond with Val143, and Val121, and Pi-Pi Stacked interaction with His94, while S7 formed conventional hydrogen bond with Thr200, His119, His94, His96, and Thr199, Pi-sigma interaction with Leu198, and Pi-sulfur interaction with Trp209. Interestingly, these results show that all the selected leads shared the same pocket and interacted favourably with the active site of the **4LU3** receptor. Summarily, it is also established that the selected leads bind to the active site of the two targets whose active site amino residues are the same, thus, it is no doubt that the selected leads C6, C13, C16, C18, C36, C45, and C49 are probable inhibitors of the Carbonic anhydrases (CAs) VII and XIV receptors which are important drug target in the discovery and development of novel anti-epilepsy medication. However, further analyses such as molecular dynamics simulation of the docked complexes to investigate the stability of the lead in the active site of the receptor at an acceptable time frame are highly recommended.

Research Through Innovation

LIGAND	C6	C13	C16	C18	C36	C45	C49	S4	S7
Formula	C ₁₉ H ₂₁ NO ₄	C ₁₅ H ₁₄ O ₆	C ₂₀ H ₂₀ NO ₄ ⁺	C ₁₉ H ₂₁ NO ₄	C ₁₉ H ₂₁ NO ₄	C ₁₃ H ₁₈ O ₇	C ₁₅ H ₂₄ O ₃	C ₁₃ H ₁₈ N ₂ O ₃	C ₄ H ₆ N ₄ O ₃ S ₂
VINA Score	-7.3(3HS4)	-7.4(3HS4)	-8.0 (3HS4)	-7.5(3HS4)	-7.1(3HS4)	-7.4(3HS4)	-7.6(3HS4)	-7.1 (3HS4)	-6.4 (3HS4)
	-	-	-7.2 3ML5)	-	-	-	-	-6.9 3ML5)	-6.4(3ML5)
	7.7(3ML5)	7.5(3ML5)	-7.4 (4LU3)	7.7(3ML5)	7.3(3ML5)	7.3(3ML5)	6.9(3ML5)	-6.7 (4LU3)	-6.4 (4LU3)
	-7.4(4LU3)	-7.8(4LU3)		-7.6(4LU3)	-7.6(4LU3)	-7.3(4LU3)	-7.5(4LU3)		
Molecular weight	327.37	290.27	338.38	327.37	327.37	286.28	252.35	250.29	222.25
#Rotatable bonds	2	1	3	2	2	4	1	8	3
XLOGP3	2.62	0.36	3.42	2.59	1.95	-1.22	1.73	0.27	-0.26

Lead likeness	0	0	0	0	0	0	0	1	1
#violations								Rotors>7	MW<250

Table 6 Lead-likeness of the selected compounds and standards

** Lead Likeness Rule: $250 \leq MW \leq 350$, $XlogP \leq 3.5$, Number of rotatable bonds ≤ 7

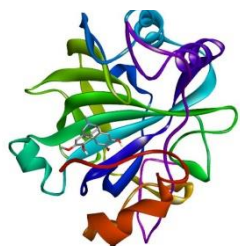
C6- Bisnorargemonine, **C13-**Catechin, **C16-**Columbamine, **C18-**Coreximine, **C36-**Pallidine, **C45-**Salicin. **C49-** alpha-carissanol, **S4-**Lacosamide, **S7-** Acetazolamide

Table 7 PASS analysis of the selected lead and standards

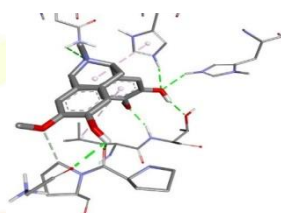
S/N	Ligands	Pa	Pi	Activity
1	Catechin (C13)	0.810	0.003	Antioxidant
		0.548	0.044	Anti-inflammatory
		0.349	0.075	GABA aminotransferase inhibitor
		0.069	0.055	NMDA receptor glycine site B antagonist
2	Bisnorargemonine (C6)	0.340	0.081	GABA aminotransferase inhibitor
		0.195	0.058	Antioxidant
		0.147	0.081	GABA C receptor antagonist
		0.226	0.169	Anticonvulsant
3	Coreximine (C18)	0.270	0.140	Anticonvulsant
		0.274	0.147	GABA aminotransferase inhibitor
		0.172	0.077	Antioxidant
		0.115	0.113	GABA C receptor antagonist
4	Salicin (C45)	0.648	0.004	Antioxidant
		0.549	0.043	Anti-inflammatory
5	Alpha-carissanol (C49)	0.302	0.113	GABA aminotransferase inhibitor
		0.219	0.046	Antioxidant
6.	Lacosamide (S4)	0.314	0.102	GABA aminotransferase inhibitor

C6 (Bisnorargemonine)

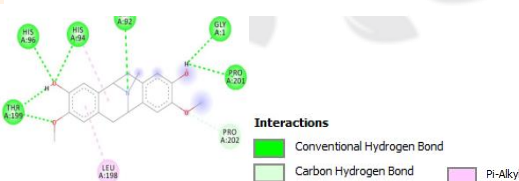
(a) 3ML5_C6 complex



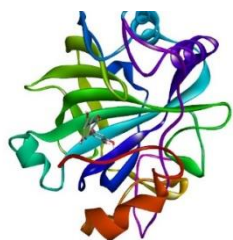
(b) 3ML5_C6 binding mode



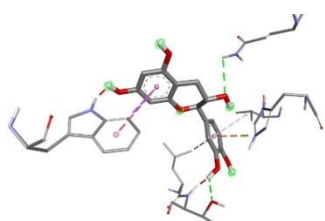
(c) 3ML5_C6 Molecular interactions

**C13 (Catechin)**

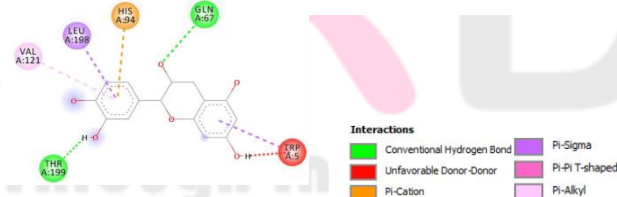
(a) 3ML5_C13 complex



(b) 3ML5_C13 binding mode



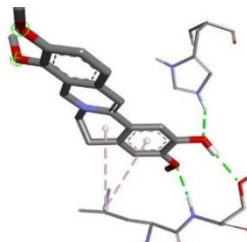
(c) 3ML5_C13 Molecular interactions

**C16 (Columbamine)**

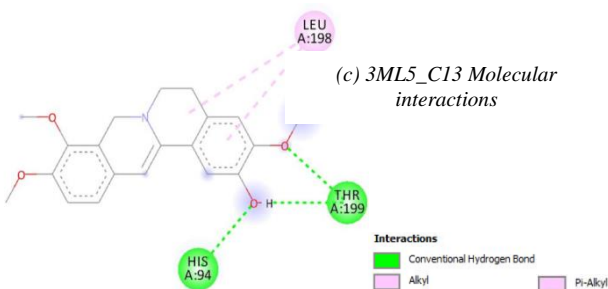
(a) 3ML5_C16 complex



(b) 3ML5_C16 binding mode

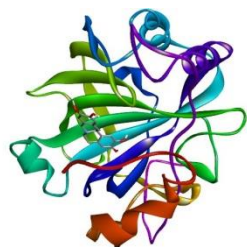


(c) 3ML5_C13 Molecular interactions

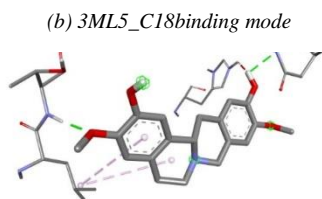
**C18 (Coreximine)**

(a) 3ML5_C18 complex

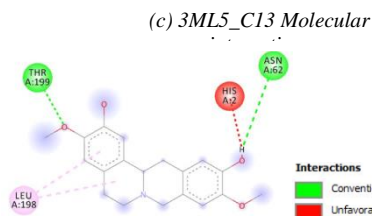




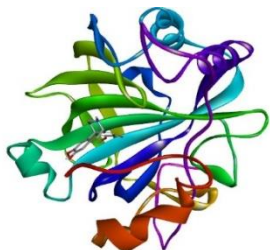
(a) 3ML5_C36 complex



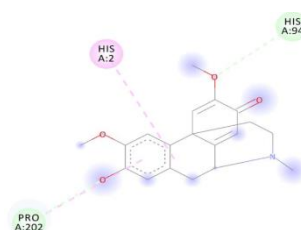
(b) 3ML5_C18binding mode



(c) 3ML5_C13 Molecular

C36 (Pallidine)

(b) 3ML5_C36binding mode



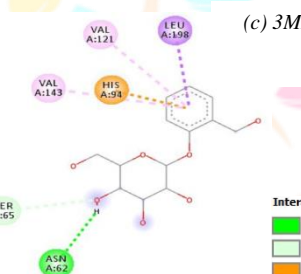
(c) 3ML5_C36 Molecular interactions

C45 (Salicin)

(a) 3ML5_C45 complex



(b) 3ML5_C45binding mode



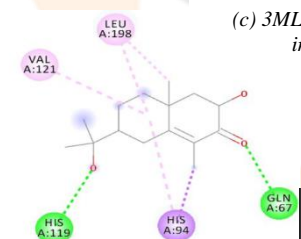
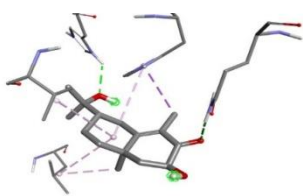
(c) 3ML5_C36 Molecular interactions

C49 (Alpha-carissanol)

(a) 3ML5_C49 complex



(b) 3ML5_C49binding mode



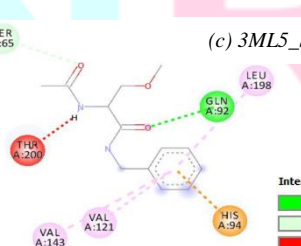
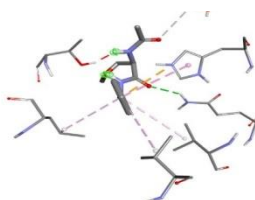
(c) 3ML5_C45 Molecular interactions

S4 (Lacosamide)

(a) 3ML5_S4 complex



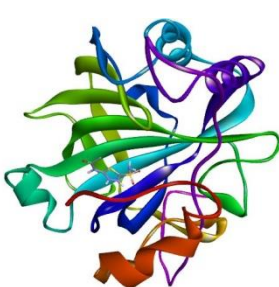
(b) 3ML5_S4binding mode



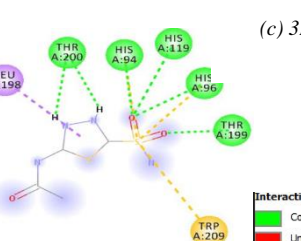
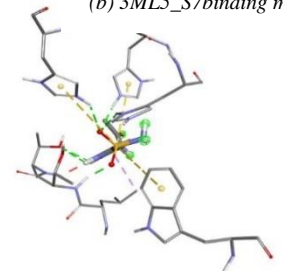
(c) 3ML5_S4 Molecular interactions

S7 (Acetazolamide)

(a) 3ML5_S7 complex



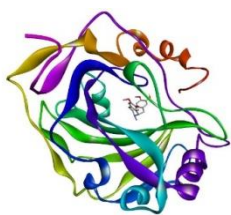
(b) 3ML5_S7binding mode



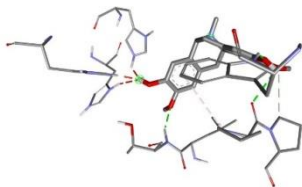
(c) 3ML5_S4 Molecular interactions

Fig. 4The binding modes and the molecular interactions of the selected leads and standards against the **3ML5** receptor**C6 (Bisnorargemonine)**

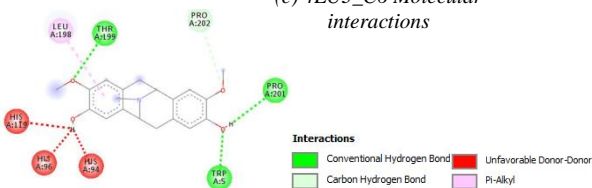
(a) 4LU3_C6 complex



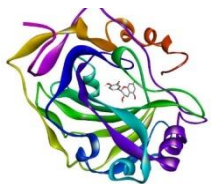
(b) 4LU3_C6 binding mode



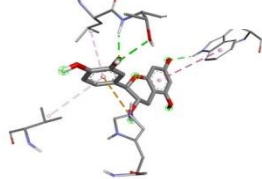
(c) 4LU3_C6 Molecular interactions

**C13 (Catechin)**

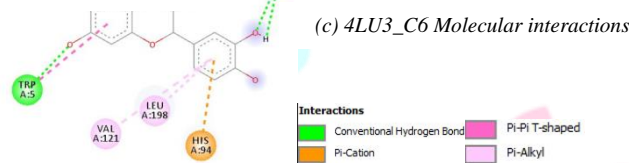
(a) 4LU3_C13 complex



(b) 4LU3_C13 binding mode



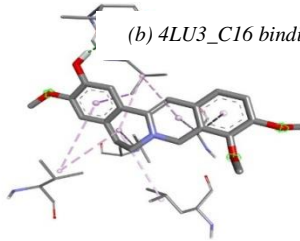
(c) 4LU3_C6 Molecular interactions

**C16 (Columbamine)**

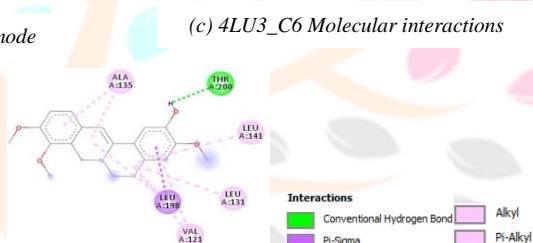
(a) 4LU3_C16 complex



(b) 4LU3_C16 binding mode



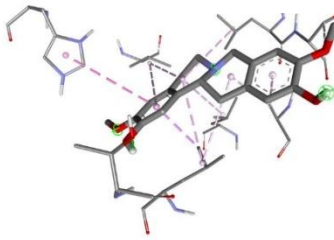
(c) 4LU3_C6 Molecular interactions

**C18 (Coreximine)**

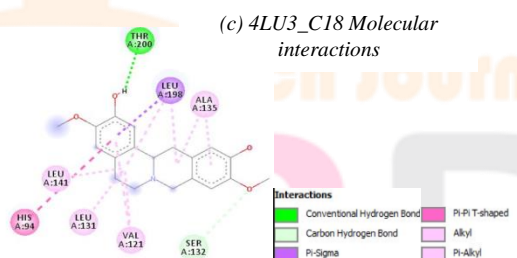
(a) 4LU3_C18 complex



(b) 4LU3_C18 binding mode



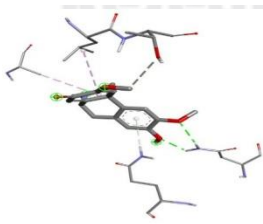
(c) 4LU3_C18 Molecular interactions

**C36 (Pallidine)**

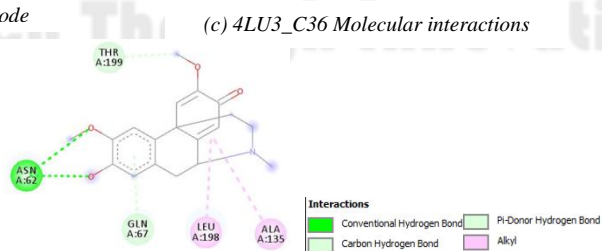
(a) 4LU3_C36 complex



(b) 4LU3_C36 binding mode



(c) 4LU3_C36 Molecular interactions

**C45 (Salicin)**

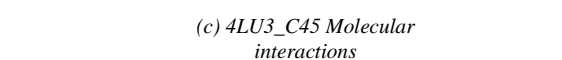
(a) 4LU3_C45 complex

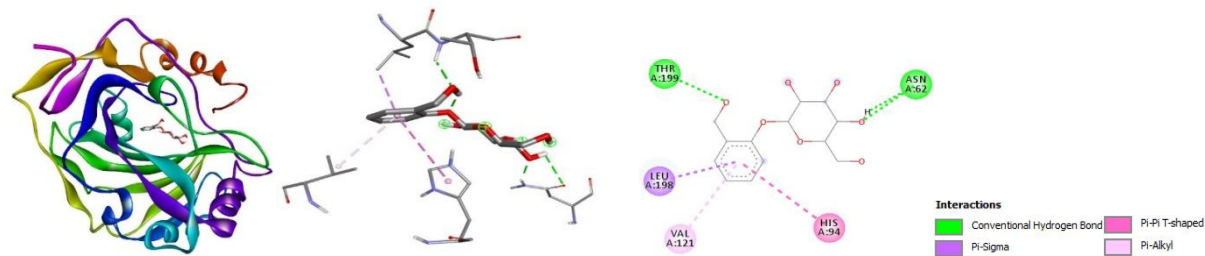


(b) 4LU3_C45 binding



(c) 4LU3_C45 Molecular interactions



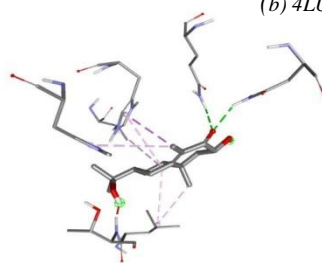
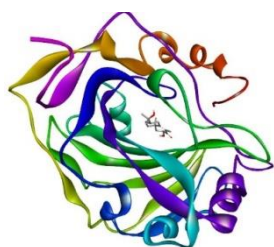


C49 (*Alpha-carissanol*)

(a) 4LU3_C49 complex

(b) 4LU3_C49 binding

(c) 4LU3_C49 Molecular interactions



Interactions

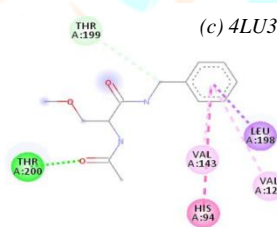
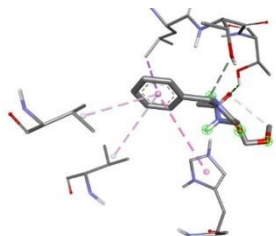
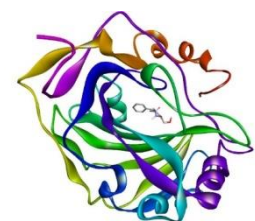
- Conventional Hydrogen Bond
- Unfavorable Donor-Donor
- Pi-Sigma
- Pi-Pi T-shaped
- Pi-Alkyl

S4 (*Lacosamide*)

(a) 4LU3_S4 complex

(b) 4LU3_S4 binding mode

(c) 4LU3_S4 Molecular interactions



Interactions

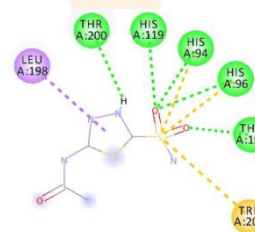
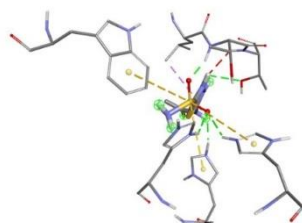
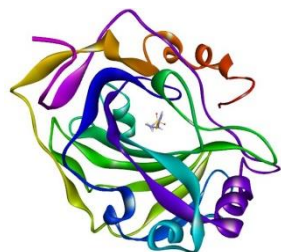
- Conventional Hydrogen Bond
- Unfavorable Donor-Donor
- Pi-Sigma
- Alkyl
- Pi-Alkyl

S7 (*Acetazolamide*)

(a) 4LU3_S7 complex

(b) 4LU3_S7 binding mode

(c) 4LU3_S7 Molecular interactions



Interactions

- Conventional Hydrogen Bond
- Carbon Hydrogen Bond
- Pi-Sigma
- Unfavorable Donor-Donor
- Pi-Sulfur

Fig. 5 The binding modes and molecular interactions of the selected leads and standards against the 4LU3 receptor

Conclusion

Epilepsy remains an unmet medical disease that requires urgent attention. Despite the availability of many commercial anti-epilepsy medications, the war against this life-threatening disease remains undefeated, thus, an urgent need for reliable lead compounds to arrest this disease remains a necessity. *In-silico* method of drug discovery helps to speed up lead identification and optimization toward the development of a reliable and highly potent novel medication and has been widely adopted in modern drug discovery operations. The current study used an *in-silico* approach (molecular docking) via a virtual screening tool (PyRx) to identify seven lead compounds capable of inhibiting the Carbonic anhydrases (CAs) VII and XIV receptors which are indispensable drug targets in anti-epilepsy drug research. The identified leads are C6-Bisnorargemonine, C18-Coreximine, C13-Catechin, C36-Pallidine, C45-Salicin, C16-Columbamine, C49- alpha-carissanol for both **3ML5** and **4LU3** receptors. In both cases, the identified leads have better binding affinities than the two standards (S4 and S7), share the same pocket with active sites of the receptors and interact favourably to give the required potency against the targets. Moreover, all the selected leads possess reliable drug-likeness, oral bioavailability, lead-likeness and PASS properties. Additionally, they all possessed ADMET profiles. Thus, the identified leads are probable inhibitors of **3ML5** and **4LU3** drug targets and could be developed further towards the development of novel and reliable anti-epilepsy drugs.

References

- Abdul-Hammed M, Adedotun IO, Falade VA, Adepoju AJ, Olasupo SB, Akinboade MW (2021) Target-based drug discovery, ADMET profiling, and bioactivity studies of antibiotics as potential inhibitors of SARS-CoV-2 main protease (M^{pro}). *Virus Dis.* 1:1-15.
- Abdul-Hammed M, Adedotun IO, Olajide M, Irabor CO, Afolabi TI, Gbadebo IO, Rhyman, L, Ramasami, P (2021) Virtual screening, ADMET profiling, PASS prediction, and bioactivity studies of potential inhibitory roles of alkaloids, phytosterols, and flavonoids against COVID-19 main protease (M^{pro}). *Natural Product Research* 1-8.
- Adedotun IO, Abdul-Hammed M, Hamzat BA, Adepoju AJ, Akinboade MW, Afolabi TI, Ismail UT (2022) Molecular docking, ADMET analysis, and bioactivity studies of phytochemicals from *phyllanthus ninuri* as potential inhibitors of hepatitis C virus NS5B polymerase. *Journal of the Indian Chemical Society* 99: 1-8.
- Adegbola PI, Semire B, Fadahunsi OS and Adegoke AE (2021) Molecular docking and ADMET studies of *Allium cepa*, *Azadirachta indica* and *Xylopi aethiopica* isolates as potential anti-viral drugs for Covid-19. *VirusDisease*. <https://doi.org/10.1007/s13337-021-00682-7>
- Adegbola PI, Fadahunsi OS, Adegoke AE and Semire B, (2021) In silico studies of Potency and safety assessment of selected trial drugs for the treatment of COVID-19. In *Silico Pharmacology* 9:45 <https://doi.org/10.1007/s40203-021-1600105-x>
- Aggarwal M, Kondeti B, McKenna R. (2013) Anticonvulsant/Antiepileptic Carbonic Anhydrase Inhibitors: A Patent Review. *Expert Opin. Ther. Patents* 23:717-724.
- Alterio V, Pan P, Parkkila S, Buonanno M, Supuran CT, Monti SM, De Simone (2013) The Structural Comparison Between Membrane-Associated Human Carbonic Anhydrases Provides Insights into Drug Design of Selective Inhibitors. *Wiley Periodicals, Inc. Biopolymers* 101:770-778.
- Beghi E (2020). The Epidemiology of Epilepsy. *Neuroepidemiology*.54:185-191.
- BIOVIA (2019). Discovery Studio Modeling Environment. San Diego: DassaultSystèmes.
- Ciccone L, Cerri C, Nencetti S, Orlandini E (2021). Carbonic Anhydrase Inhibitors and Epilepsy: State of the Art and Future Perspectives. *Molecules*. 26:1-18.
- Daina A, Michielin O, Zoete V (2017). SwissADME: A free web tool to evaluate the pharmacokinetics, drug-likeness, and medicinal chemistry friendliness of small molecules. *Sci Rep*.7:42717.
- Devinsky O, Vezzani A, O'Brien TJ, Jette N, Scheffer IE, De Curtis M, Perucca P (2018). Epilepsy. *Nat. Rev. Dis. Prim.* 4:18024.
- Di Fiore A, Truppo E, Suporan CT, Alterio V, Dathan N, Bootorabi F, Parkkila S, Monti SM, De Simone G (2010) Crystal structure of the C183S/C217S mutant of human CA VII in complex with acetazolamide. *Bioorg.Med.Chem.Lett.* 20:5023-5026.
- Engel J (2001). Mesial Temporal Lobe Epilepsy: What Have We Learned? *Neuroscientist*.7: 340-352.

Falade VA, Adelusi TI, Adedotun IO, Abdul-Hammed M, Lawal TA and Agboluaje SA (2021). In-silico investigation of saponins and tannins as potential inhibitors of SARS-CoV-2 main protease (M^{pro}). In *Silico Pharmacology*. 9:1-15.

Goel RK, Singh D, Lagunin A, Poroikov V (2011). PASS-assisted exploration of new therapeutic potential of natural products. *Med Chem Res.*20: 1509-1514.

Guan L, Yang H, Cai Y, Sun L, Di P, Li W, Liu G, Tang Y (2018). ADMET-score - a comprehensive scoring function for evaluation of chemical drug-likeness. *Med. Chem. Comm.* 30:148-157.

Kalilani L, Sun X, Pelgrims B, Noack-Rink M, Villanueva V (2018). The epidemiology of drug-resistant epilepsy: A systematic review and meta-analysis. *Epilepsia*. 59: 2179-2193.

Krishnamurthy, VM, Kaufman, GK, Urbach, AR, Gitlin I, Gudiksen KL, Weibel DB, Whitesides GM (2008) *Chem. Rev.* 108: 946-1051.

Kwan P (2004). The natural history of epilepsy: An epidemiological view. *J. Neurol. Neurosurg. Psychiatry*. 75: 1376-1381.

Kwan P, Arzimanoglou A, Berg AT, Brodie MJ, Hauser WA, Mathern G, Moshé SL, Perucca E, Wiebe S, French J (2009). Definition of drug-resistant epilepsy: Consensus proposal by the ad hoc Task Force of the ILAE Commission on Therapeutic Strategies. *Epilepsia*.51: 1069-1077.

Leniger T, Thöne J, Wiemann M (2004). Topiramate Modulates pH of Hippocampal CA3 Neurons by Combined Effects on Carbonic Anhydrase and Cl⁻/HCO₃⁻Exchange. *Br. J. Pharmacol.* 142: 831-842.

Lipinski CA (2004). Lead profiling Lead- and drug-like compounds: The rule-of-five revolution. *Drug Discovery Today: Technologies*. 1: 337–341.

Löscher W, Potschka H, Sisodiya SM and Vezzani A (2020). Drug Resistance in Epilepsy: Clinical Impact, Potential Mechanisms, and New Innovative Treatment Options. *Pharmacol. Rev.*72: 606-638.

Mishra CB, Tiwari M, Supuran CT (2020). Progress in the Development of Human Carbonic Anhydrase Inhibitors and their Pharmacological Applications: Where Are We Today? *Med. Res. Rev.* 40: 2485-2565.

Onawole AT, Sulaiman KO, Adegoke RO, Kolapo TU. 2017. Identification of potential inhibitors against the Zika virus using consensus scoring. *J Mol Graph Model*. 73:54–61.

Oyebamiji AK, Oladipo EK, Olotu TMI, Awoyelu HE, Adamolekun E and Semire B (2020) In-vitro Investigation on Selected compounds in Annona Muricata Seed: A Potential SARS-CoV
Polymerase Inhibitors down Regulating 2019-nCoV. *International Journal of Traditional and Natural Medicines*, 10(1): 13-23

Oyebamiji AK, Olujinmi FE, Akintayo ET, Akintayo CO, Akintelu SA, Semire B, Babalola JO, Okunlola F, and Olawoye BM (2023) Potential Inhibiting Activities of Phytochemicals from Enantia chlorantia Bark Against Lactate Dehydrogenase: in Silico Approach. *Eurasian Journal of Chemistry*.
<https://doi.org/10.31489/2959-0663/4-23-2>

Ozsoy HZ (2021). Anticonvulsant Effects of Carbonic Anhydrase Inhibitors: The Enigmatic Link Between Carbonic Anhydrases and Electrical Activity of the Brain. *Neurochem. Res.*46: 2783-2799.

Pitkänen A, Lukasiuk K (2011). Mechanisms of epileptogenesis and potential treatment targets. *Lancet Neurol.* 10: 173-186.

Ramachandran GN, Sasisekharan V (1968). Conformation of Polypeptides and Proteins. *Advances in Protein Chemistry* 23: 283-437.

Ruusuvuori E, Kaila K (2014). Carbonic Anhydrases and Brain pH in the Control of Neuronal Excitability. In *Carbonic Anhydrase: Mechanism, Regulation, Links to Disease, and Industrial Applications*; Frost, S.C., McKenna, R., Eds.; Subcellular Biochemistry. Springer: Dordrecht, The Netherlands. pp. 271-290.

Sanguinetti MC, Tristani-Firouzi M (2006). hERG potassium channels and cardiac arrhythmia. *Nature*.440: 463-469.

Sarmast ST, Abdullahi AM, Jahan N (2020). Current Classification of Seizures and Epilepsies: Scope, Limitations, and Recommendations for Future Action. *Cureus*. 12: e10549.

Sippel KH, Robbins AH, Domsic J, Genis C, Agbandje-Mckenna M, McKenna R (2009). The high-resolution structure of human carbonic anhydrase II complexed with acetazolamide reveals insights into inhibitor drug design. *Structural Biology and Crystallization Communications*.F65: 992-995.

Supuran, CT (2010). Carbonic Anhydrase Inhibitors. *Bioorganic Med. Chem. Lett.*20: 3467-3474.

Tian W, Chen C, Lei X et al (2019). CASTp 3.0: computed atlas of surface topography of proteins. *Nucleic Acids Res*46: W363–W367

Tong CK, Cammer W, Chesler M (2000). Activity-dependent pH Shifts in Hippocampal Slices from Normal and Carbonic Anhydrase II-Deficient. Mice. *Glia*.31: 125-130.

Tsaoun KS (2011). ADMET for medicinal chemists: A practical guide. New Jersey: Wiley.

William OA, Ejike OO , Obiyenwa KG , Godfrey OE and Semire B (2024) Phytochemical screening, anti-proliferative evaluation, and molecular docking studies of *Acacia nilotica* fruit from Nigeria. *Ecletica Quimica*. 49, e-1512, <https://doi.org/10.26850/1678-4618.eq.v49.2024.e1512>

Yang H, Lou C, Sun, L *et al.* (2019). “AdmetSAR 2.0: Web-service for prediction and optimization of chemical ADMET properties”. *Bioinformatics* 35: 1067-1069.

Yaro JAH, Malami S, Musa MA, Abubakar A, Yahaya SM, Chindo BA, Anuka JA, Hussaini IM (2015) Anticonvulsant activity of aqueous fraction of *Carissa edulis* root bark, *Pharmaceutical Biology*. 53: 1329-1338.

Zavala-Tecuapetla C, Cuellar-Herrera M, Luna-Munguia H (2020). Insights into Potential Targets for Therapeutic Intervention in Epilepsy. *International Journal of Molecular Sciences* .21: 1-54.

